

ABSTRACT

LIGHTWALA, HUZEFA MURTUZA. Least Effort Tracking Model for the Motion Planning of a Tarantula Robot. (Under the direction of Dr. Lawrence Silverberg).

Legged robots are adaptable to uneven terrain and well suited for navigation and exploration. However, their advanced maneuverability comes at the cost of complex inverse kinematics and motion planning algorithms. We address the motion planning for walking application of a tarantula robot. A tarantula is an 8-legged arthropod with a high degree of redundancy, rendering it with several motion choices while walking. To interpret these choices, we present a hierarchical approach which breaks down the problem into small parts and gain insight into them. The information derived is used to holistically develop the walking gaits of a tarantula robot moving on flat ground. We leverage the least effort principle (the basis for usual motions of animals) for making motion planning decisions. Furthermore, we compare our derived gaits with those exhibited by tarantulas (using available videos and previous research). Our comparative studies found close resemblance between the two. This may suggest that the least effort principle plays an important role in the decision-making process of the tarantula while walking. A [video](#) of the final walking motion is available on YouTube.

© Copyright 2021 by Huzefa Murtuza Lightwala

All Rights Reserved

Least Effort Tracking Model for the Motion Planning of a Tarantula Robot

by
Huzefa Murtuza Lightwala

A thesis submitted to the Graduate Faculty of
North Carolina State University
in partial fulfillment of the
requirements for the degree of
Master of Science

Mechanical Engineering

Raleigh, North Carolina
2021

APPROVED BY:

Dr. Lawrence Silverberg
Committee Chair

Dr. Gregory Buckner

Dr. John-Paul Ore

BIOGRAPHY

Huzefa was born in Mumbai, India and has been pursuing his career and lifelong dream in mechanical engineering. He moved to the US in 2019 for pursuing his master's in mechanical engineering and had a chance to experience several triumphs as well as sorrows, both inside and outside the classroom. However, each new experience taught him to be a better human and brought him one step closer to living a better life. This thesis was one of his biggest accomplishments and hopefully, he contributed towards science and humanity which is perhaps the biggest success of the thesis.

ACKNOWLEDGMENTS

Writing a thesis is not only a challenge for your acumen but also for your patience, courage, and the general ability to keep yourself together. Even though this thesis has my name at the beginning, it would be impossible to achieve without the support of certain important people in my life. I would like to thank each of them starting with the most beloved two, my mother and my father. During the entire duration of the thesis, I was thousands of miles from home, but they managed to keep me going though all thick and thin. I would like to thank the rest of my family including my sister and grandparents, especially my grandfather, who I lost this year but would never stop being proud of me.

I would like to thank Dr. Silverberg for firstly teaching me so much and secondly, walking me through the wonderful subject of dynamics and control. There were several moments when I doubted my own work, but he encouraged me to never stop believing and listened patiently to my silliest ideas and concepts.

I would also like to thank the rest of my committee, Dr. Gregory Buckner and Dr. John-Paul Ore for firstly agreeing to be part of the venture and next for teaching two of the best courses at NC State University. Their insightful lectures helped me throughout my thesis.

Lastly, I would like to thank my friends- Suchit, Shravan, Keerti, Vaibhav, Ankit and several others and I am grateful for the innumerable laughs we shared during these 2.5 years that helped me subdue the stress of academics. They were my family, several miles away from home.

Thank you everyone!

TABLE OF CONTENTS

LIST OF TABLES	v
LIST OF FIGURES	vi
1. Introduction.....	1
2. Methodology.....	5
2.1 Spider kinematic model	6
2.2 Kinematics	7
2.3 Dynamics	10
2.4 Leg in the air phase (The swing phase):	12
2.5 Leg on the ground phase (The stance phase)	17
2.6 Calculating the normal forces:	19
2.7 Calculating the ground plane forces (Least-effort Problem 3 or LEP 3):.....	21
2.8 The Final Optimization Problem	22
3. Results.....	29
3.1 Least-effort Problem 1 Results:	29
3.2 Least-effort Problem 2 and 3 Results:	31
3.3 The Final Optimization Problem Results:.....	35
4. Conclusions.....	43
REFERENCES	44

LIST OF TABLES

Table 1:	Physical quantities for the tarantula model	6
Table 2:	Joint Constraints used throughout the paper	7
Table 3:	List of all parameters used in the FOP	25
Table 4:	Optimization results for stride length of 0.035m	37
Table 5:	Optimization results for stride length of 0.038m	38

LIST OF FIGURES

Figure 1: Model of the Tarantula	5
Figure 2: Joint angles and leg plane of a single leg	8
Figure 3: Free body diagram of a single link	9
Figure 4: The four parameters used to define the leg configuration.....	13
Figure 5: Equivalent spring mass system of the spider with n legs in contact with the ground ...	19
Figure 6: Illustration of various notable parameters used in the FOP	23
Figure 7: Flowchart of the procedure of calculating the objective function for the FOP.....	28
Figure 8: Series of images showing a leg flexing for same initial and final conditions.....	30
Figure 9: Least effort leg configurations derived from LEP 2.....	32
Figure 10: The θ_{1max} configuration region is illustrated for two foot positions.....	32
Figure 11: Variation of the optimal ground plane force with Leg radius and Normal force	33
Figure 12: Demonstration of optimal ground plane forces derived from LEP 3	34
Figure 13: Leg position maps when the last leg of the leg group contacts the ground.....	39
Figure 14: Gait phase diagrams of tarantulas from 4 different sources.....	41
Figure 15: Joint angles during the walking gait cycle for legs R1, R2, R3 and R4.....	42

1. Introduction

Legged robots, such as bipeds, quadrupeds, and six and eight legged systems, have been the subject of scientific research for many years. Perhaps the most frequent advantage cited is their ability to traverse on uneven terrain and overcome obstacles, which makes them well suited to exploration, hard to reach locations, and outdoor navigation. Perhaps the largest disadvantage arises from the complexity of the motion planning and control, particularly when compared to wheeled robots. This complexity results from the relatively large number of interconnected links, which, in turn, produces redundancy. Indeed, many legged systems are composed of more degrees of freedom than are necessary to ambulate in three-dimensional space, resulting in an infinite number of paths associated with a task.

One of the common ways to circumvent the problem of redundancy and avoid the need for complex motion planning is to emulate the motions of animals. This is done through imitation learning wherein; the robot is demonstrated the motions it needs to perform by a teaching agent [1]. It works by instrumenting an animal with sensors and monitoring its motion. This approach becomes problematic when it is difficult to instrument the animal with sensors, particularly when the animal is small, like in insects and arachnids. Furthermore, it is difficult to monitor every kind of motion, which makes it difficult to translate the monitored data into feedback control algorithms and additional approaches such as reinforcement learning are needed for deriving the motions every time the task is even minutely different than the recorded one. [2].

To overcome the before mentioned redundancy problem, one typically derives end effector paths and/or the inverse kinematics of robot links by minimizing or constraining physical parameters

such as time, joint torque, joint velocity, and energy consumption [3]. In [4], the authors developed a minimization problem for industrial robots that weights time consumed, joint torques, and power consumed. They used Sequential Quadratic Programming to successfully derive motions while avoiding obstacles for the PUMA 560 robot and a 3 DOF planar pick and place task. The authors of [5] explored a multi-objective optimization function that minimizes joint torques and maximizes motion smoothness, to derive heavy lifting motions while accounting for the lifter's age. They found that younger adults prioritize joint torque while older adults prioritize smooth motion when lifting heavy objects. For locomotion, the authors of [6] proposed a novel method for deriving natural looking walking motions for bipedal robots. Instead of attempting to derive the motions, they allowed the robot to perform pre-recorded reference motions, and then optimized their way through deriving different physical parameters and mechanical properties of the robot, used in literature to describe a dynamical model for a bipedal robot. Then, they used the set of derived parameters to define a "style" of walking for the robot, from which they produced more walking motions. In [7], the authors compared such optimization criteria as minimum time, least-effort, minimum angular amplitudes, and minimum head velocity in their human bipedal model.

In legged robots, it is often desirable to emulate life-like walking motion. To obtain them, one can draw inspiration from the choices animals make, consciously or not, while walking. According to [8], these choices follow a minimum principle, referred to as the least-effort principle, henceforth, which corresponds to the tendency to minimize over time total muscular effort. To map this principle to robots, one can minimize over time the total joint torques, because they are proportional to muscular tension [8]. While in depth models have been suggested to translate from the muscle actuation space to the joint actuation space [9], researchers have often relied on simply

minimizing joint torques over time in their mechanical robot models, to obtain motions for robot manipulation as well as for locomotion [10] [11] [12]. We plan to use a similar method to determine motions for a tarantula robot walking on a flat surface.

The tarantula is a fairly large and benign type of spider that is abundant in nature. Its primary mode of locomotion is ground ambulation and, with eight legs and four joints per leg, it has high mobility and is able to walk on uneven terrain. Hair like *setae* and claws on their feet and silk weaving legs allow them to walk vertically and climb upside down, too. These walking capabilities make them a good choice for bio-inspired robots, especially for exploration. Furthermore, the intricate coordination between their eight legs generates fascinating walking patterns. If one were able to reproduce their walking behavior, they could even be a great choice for toy robots. More generally, though, they would have value to younger and older people alike [13] [14] [15].

While spiders are ubiquitous, it appears that the literature has little about 8-legged robots, as well as their habitual motion. Also, to the best of our knowledge, no work intends for the robot to resemble an actual spider. A notable mention is the T8X by Robugtrix [16] which may be the only robot on the market that closely replicates an actual spider. However, no literature about the motion planning of this robot is available. Moreover, this robot model treats the *Tibia-Metatarsus* joint as a rigid joint. The robot also does not capture certain attributes of an actual tarantula such as the alternating tetrapodal gait. Our first objective was to demonstrate with the help of the least-effort principle, a hierarchical framework that can produce life-like motions for a dynamical model – bearing close resemblance to a tarantula spider walking on a flat surface. Not only does a tarantula have redundant legs, but it also has redundant joints along each leg, which makes it highly

adaptable to the different walking conditions – at the expense of complex motion planning. This may be one of the reasons why the existing 8-legged robots [17],[18],[19],[20],[21] were simplified versions of a tarantula with either lesser degrees of freedom in the legs or without the objective of retaining the life-like motions and resemblance of animals. Hence, in this article we will adopt the hierarchical approach – to break down the bio-inspired model of the tarantula into its elements, starting from a link to a leg and then to the whole spider. This framework can be further extended to develop more general motions for the spider such as walking on uneven surfaces or sloped surfaces or jumping among others. Our second objective is to gauge the role of least-effort in the motions that the tarantula chooses to make while walking. While tarantulas demonstrate a number of variations of walking that depend on ground conditions, certain attributes are consistently reported by biologists that have studied tarantula motion [22],[23],[24]. Hence, we aim derive such attributes using the least-effort principle and compare them with those performed by an actual spider to see how well the theory is able to predict a tarantula’s motion planning process while walking.

2. Methodology

This section develops a heuristic for deriving the walking motion of a tarantula. We first define a general kinematic model for the entire spider (2.1) and then we divide the spider into subsections. We start with deriving general dynamic equations for a single link (2.2, 2.3) and then move on to solving least-effort optimization problems to derive certain parameters for a single leg. A leg may have two phases—it may be swinging in the air or in contact with the ground. Each case is considered separately in 2.4 and 2.5. When the leg is in contact with the ground, certain forces are developed at the foot, and these forces are investigated in 2.6 and 2.7. The parameters derived in all these sections aid in reducing certain unknowns when studying the entire spider. Walking gaits are then derived at the end of this section (2.8) using information and parameters from the subsections above.

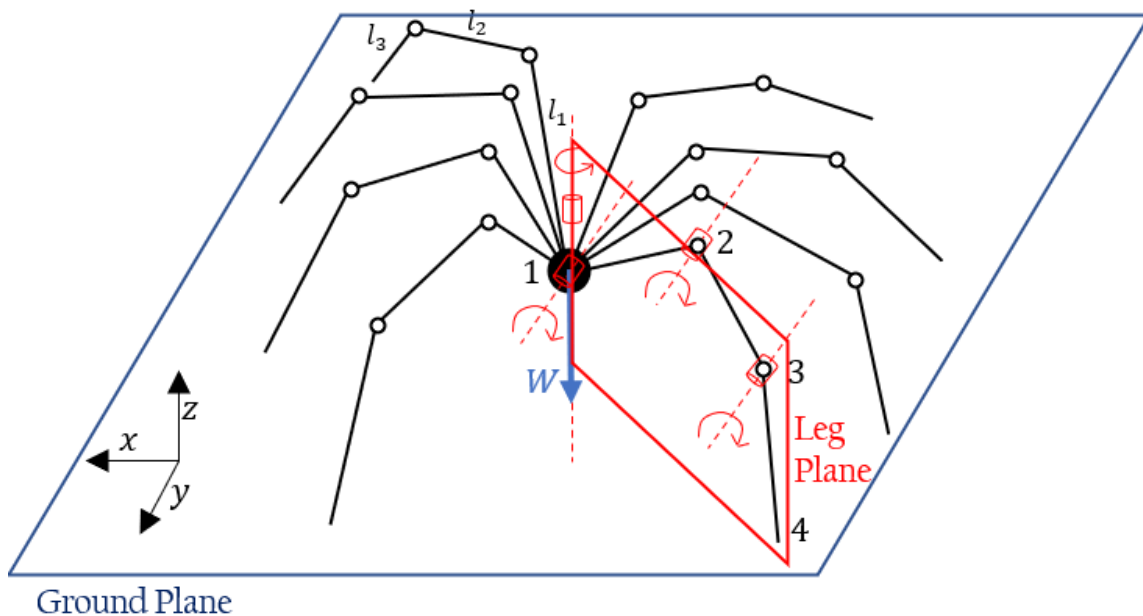


Figure 1: Model of the Tarantula.

2.1 Spider kinematic model

A tarantula has 8 legs for walking and 2 pedipalps that also aid in walking along with other functions [25]. In our model, as in [26], we neglect the role of pedipalps in walking. The body is modeled as a point mass and the leg is a 3-link planar system connected to the body through a revolute joint that lets the leg rotate about an axis normal to ground (See Fig. 1). The plane holding the 3 links of each leg defines a leg plane, and within the leg are 3 revolute joints that allow it to flex, extend and rotate within the leg plane. Hence, the revolute joint connecting a leg to the point mass is the only joint that allows the leg to move out of plane. In all, the spider model consists of 24 links and 32 joints. Some physical parameters of the spider model are given below Literature on tarantulas is sparse and the parameters were chosen based on data available in [24] [27] [28].

Table 1: Physical quantities for the tarantula model.

Physical quantity	Value	Unit	Variable
Spider Body mass (<i>Cephalothorax</i> and abdomen, <i>coxa</i> , <i>pedipalps</i> and <i>chelicerae</i>)	0.033	kg	M
Spider leg link 1 length (<i>Trochanter</i>)	0.025	m	l_1
Spider leg link 2 length (<i>Patella-Tibia</i>)	0.025	m	l_2
Spider leg link 3 length (<i>Tarsus-Metatarsus</i>)	0.025	m	l_3
Link 1 mass	0.00053	kg	m_1
Link 2 mass	0.00053	kg	m_2
Link 3 mass	0.00053	kg	m_3
Total mass of the Spider	0.0457	kg	M_T
Total weight of the Spider	0.4485	N	W

2.2 Kinematics

We assume that the leg plane is upward and that the ground plane is horizontal and define an inertial frame $\{L\}$ at the body in which the z axis always points upward and the x axis is instantaneously coincident with the leg plane and points to the right from the body towards the foot. The leg plane angle, which is denoted by ϕ , is about the z axis and the joint angles of a leg are about the y axis (See Fig. 2). As shown ϕ follows a right-hand rule; it is positive when the rotation about the z axis is positive. The other joint angles follow a left-hand rule; they are positive when the rotation about y is negative. The joints of a spider have physical limits and throughout the paper, we use joint constraints to represent these limits [25]. The joint constraints used are shown in table 2.

Table 2: Joint Constraints used throughout the paper,

Joint Constraint	Physical significance
$\theta_1 \leq 90^\circ$	<i>Femur</i> or Link 1 does not collide with the body.
$\theta_2 \leq \theta_1$	Physical limit of the <i>Femur-Patella</i> joint or joint 2 (Refer Fig. 2).
$\theta_3 \leq \theta_2$	Physical limit of the <i>Tibia-Metatarsus</i> joint or joint 3 (Refer Fig. 2).
$z_4 \geq \textit{Spider height}$	Avoids collision of the foot with the ground.
ϕ of a leg $>$ ϕ of all legs on its posterior side	Avoids collision of Legs

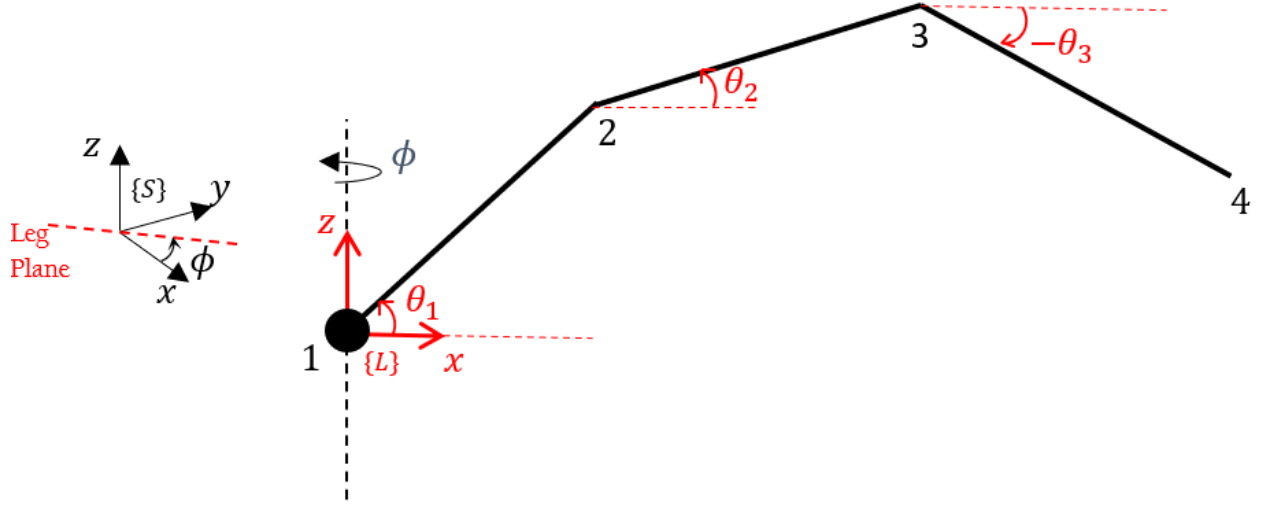


Figure 2: Joint angles and leg plane of a single leg.

In the leg frame $\{L\}$, the joint coordinates are

$$x_n = x_{n-1} + l_{n-1} \cos(\theta_{n-1}), \quad y_n = y_{n-1}, \quad z_n = z_{n-1} + l_{n-1} \sin(\theta_{n-1})$$

$$(n = 2, 3, 4)$$

Transforming to the Stationary frame $\{S\}$ yields

$$\begin{pmatrix} x_n \\ y_n \\ z_n \end{pmatrix}_{\{S\}} = \begin{pmatrix} x_1 \\ y_1 \\ z_1 \end{pmatrix}_{\{S\}} + \begin{bmatrix} \cos(\phi) & -\sin(\phi) & 0 \\ \sin(\phi) & \cos(\phi) & 0 \\ 0 & 0 & 1 \end{bmatrix} \begin{pmatrix} x_n \\ y_n \\ z_n \end{pmatrix}_{\{L\}}$$

Next, consider a single link, letting 1 and 2 designate its end-points (See Fig. 3). Indeed, we let $x_1(t), x_2(t), y_1(t), y_2(t), z_1(t), z_2(t)$ refer to the coordinates of the end-points in $\{S\}$. The x coordinate of the mass center (denoted by C) of the link is

$$x_c(t) = \frac{x_1(t) + x_2(t)}{2}$$

Similar equations apply to the other coordinate directions. Also, for the x coordinate direction of the velocity of the mass center and the acceleration of the mass center, for small ε we have

$$v_{cx} = \frac{dx_c}{dt} \cong \frac{x_c(t + \varepsilon) - x_c(t)}{\varepsilon}, \quad a_{cx} = \frac{dv_{cx}}{dt} \cong \frac{v_{cx}(t + \varepsilon) - v_{cx}(t)}{\varepsilon}$$

where, again, we have similar equations for the other coordinate directions.

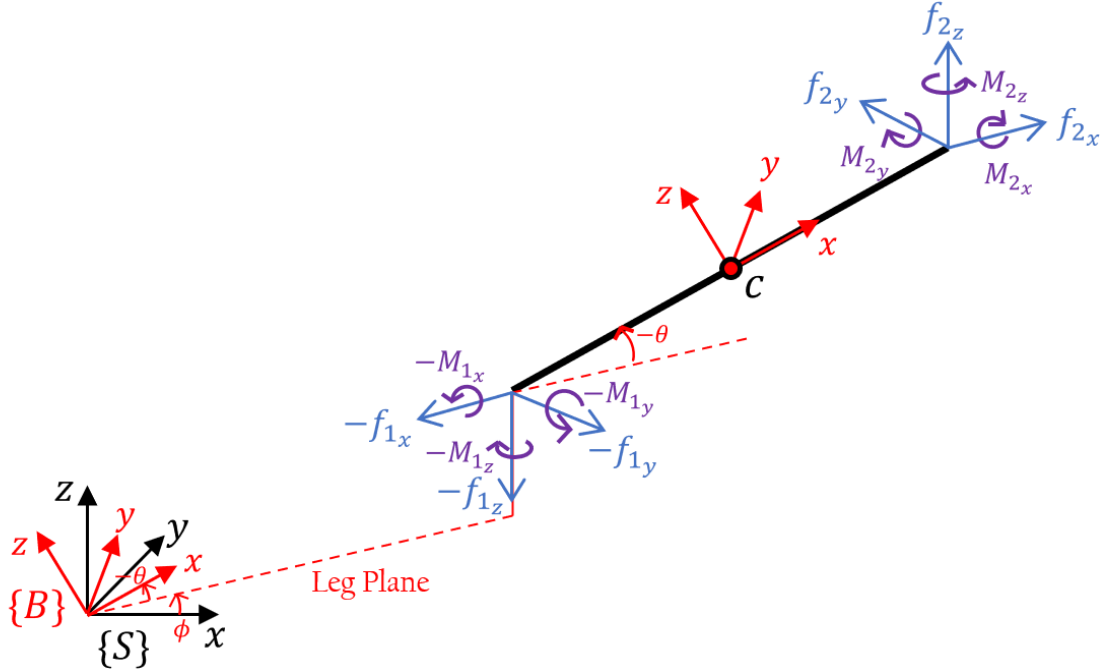


Figure 3: Free body diagram of a single link.

Next, let us define a new body frame $\{B\}$ whose origin is located at C , whose x axis is along the length of the link, and whose y axis is perpendicular to the leg plane (See Fig. 3). In the new body frame the 3×3 inertia matrix of the link is constant. The rotation matrix of the new frame is

$$R(-\theta, \phi) = \begin{bmatrix} \cos(\theta)\cos(\phi) & -\sin(\phi) & \sin(\theta)\cos(\phi) \\ \cos(\theta)\sin(\phi) & \cos(\phi) & \sin(\theta)\sin(\phi) \\ -\sin(\theta) & 0 & \cos(\theta) \end{bmatrix}$$

where θ corresponds to the link. The transformation between the unit vectors is

$$\begin{pmatrix} \hat{b}_1 \\ \hat{b}_2 \\ \hat{b}_3 \end{pmatrix} = R(-\theta, \phi)^T \begin{pmatrix} \hat{s}_1 \\ \hat{s}_2 \\ \hat{s}_3 \end{pmatrix}$$

Therefore,

$$v_{C\{B\}} = R^T v_{C\{S\}}$$

$$a_{C\{S\}} = \frac{dv_{C\{S\}}}{dt} = \frac{d}{dt}(Rv_{C\{B\}}) = v_{C\{B\}} \frac{dR}{dt} + Ra_{C\{B\}}$$

so

$$a_{C\{B\}} = R^{-1}(a_{C\{S\}} - v_{C\{B\}} \frac{dR}{dt})$$

where,

$$\frac{dR(t)}{dt} \cong \frac{R(-\theta(t + \varepsilon), \phi(t + \varepsilon)) - R(-\theta(t), \phi(t))}{\varepsilon}$$

Similarly,

$$\omega_{C\{S\}} = R\omega_{C\{B\}} \quad \text{So,} \quad \alpha_{C\{B\}} = \frac{d\omega_{C\{B\}}}{dt} = R^{-1}(\alpha_{\omega_{C\{S\}}} - \omega_{\omega_{C\{B\}}} \frac{dR}{dt})$$

where,

$$\omega_{C\{B\}} = \begin{bmatrix} \dot{\phi}(t) \sin(-\theta(t)) \\ \dot{\theta} \\ \dot{\phi}(t) \cos(-\theta(t)) \end{bmatrix} = \begin{bmatrix} -\dot{\phi}(t) \sin(\theta(t)) \\ \dot{\theta} \\ \dot{\phi}(t) \cos(\theta(t)) \end{bmatrix}$$

And,

$$\alpha_{C\{S\}} \cong \frac{\omega_{C\{S\}}(t+\varepsilon) - \omega_{C\{S\}}(t)}{\varepsilon}$$

2.3 Dynamics

The governing force and moment equations are

$$F_B = m\omega_{C\{B\}} \times v_{C\{B\}} + ma_{C\{B\}}$$

$$M_B = I_B \alpha_{C\{B\}} + \omega_{C\{B\}} \times I_B \omega_{C\{B\}}$$

We can balance the forces and moments for each of the six degrees of freedom of the link using the above equations and derive general equations for any collection of forces and moments acting at the ends of each link. All force, moments and kinematic quantities will be considered in the $\{B\}$ frame as described above and we drop the $\{B\}$ subscript from here on. However, the forces are oriented along the leg frame $\{L\}$ as shown in Fig. 3 to maintain consistency in their directions by

making them independent of the link orientation as each link of the leg is analyzed one after another.

We have:

Force balance along the x, y and z axis:

$$F_{2_x}c_{-\theta} + F_{2_z}s_{-\theta} - F_{1_x}c_{-\theta} - F_{1_z}s_{-\theta} - mg.s_{-\theta} = ma_{C_x} + m(\omega_C \times v_C)_x$$

$$F_{2_y} - F_{1_y} = ma_{C_y} + m(\omega_C \times v_C)_y$$

$$F_{2_z}c_{-\theta} - F_{2_x}s_{-\theta} - F_{1_z}c_{-\theta} + F_{1_x}s_{-\theta} - mg.c_{-\theta} = ma_{C_z} + m(\omega_C \times v_C)_z$$

Moment balance about the x, y and z axes:

$$M_{2_x}c_{-\theta} - M_{1_x}c_{-\theta} + M_{2_z}s_{-\theta} - M_{1_z}s_{-\theta} = 0$$

(Since $I_x \approx 0$ for a slender link)

$$M_{2_y} - M_{1_y} + 0.5l F_{2_x}s_{-\theta} + 0.5l F_{1_x}s_{-\theta} - 0.5l F_{2_z}c_{-\theta} - 0.5l F_{1_z}c_{-\theta} = I_y\alpha_{C_y} + (\omega_C \times I\omega_C)_y$$

$$-M_{2_x}s_{-\theta} + M_{1_x}s_{-\theta} + M_{2_x}c_{-\theta} - M_{1_x}c_{-\theta} + 0.5F_{2_y}l + 0.5F_{1_y}l = I_z\alpha_{C_z} + (\omega_C \times I\omega_C)_z$$

This can be converted into a matrix and can be solved for each link starting from the farthest link from the body or link 3 to the nearest or link 1. The matrix form of above equations is:

$$\begin{bmatrix} -c_{\theta} & 0 & s_{\theta} & 0 & 0 & 0 \\ 0 & -1 & 0 & 0 & 0 & 0 \\ -s_{\theta} & 0 & -c_{\theta} & 0 & 0 & 0 \\ 0 & 0 & 0 & -c_{\theta} & 0 & s_{\theta} \\ -0.5ls_{\theta} & 0 & -0.5lc_{\theta} & 0 & -1 & 0 \\ 0 & 0.5l & 0 & -s_{\theta} & 0 & -c_{\theta} \end{bmatrix} \begin{bmatrix} F_{1_x} \\ F_{1_y} \\ F_{1_z} \\ M_{1_x} \\ M_{1_y} \\ M_{1_z} \end{bmatrix} = \begin{bmatrix} -F_{2_x}c_{\theta} + F_{2_z}s_{\theta} \\ -F_{2_y} \\ -F_{2_z}c_{\theta} - F_{2_x}s_{\theta} \\ -M_{2_x}c_{\theta} + M_{2_z}s_{\theta} \\ -M_{2_y} + 0.5l(F_{2_x}s_{\theta} + F_{2_z}c_{\theta}) \\ -M_{2_x}s_{\theta} - M_{2_z}c_{\theta} - 0.5F_{2_y}l \end{bmatrix} + \begin{bmatrix} -mgs_{\theta} \\ 0 \\ mgc_{\theta} \\ 0 \\ 0 \\ 0 \end{bmatrix} + \begin{bmatrix} m[a_C] \\ I[\alpha_C] \\ m[\omega_C \times v_C] \\ [\omega_C \times I\omega_C] \end{bmatrix}$$

or

$$\mathcal{T}(-\theta) \cdot \mathcal{F}_1 = \mathcal{F}_2 + \mathcal{W} + \mathcal{D}_1 + \mathcal{D}_2$$

We call this the matrix equation for a leg. When the spider is walking, some of its legs may be contacting the ground to support the body while the rest are swinging in the air. Thus, each leg has two states, the stance phase, when the foot of that leg is on the ground and the swing phase when

it is in the air. Each leg attains both states in a single walk cycle. We consider each of these cases separately below:

2.4 Leg in the air phase (The swing phase):

When the leg is in the air, its one end is a free end and $f_{2x} = f_{2y} = f_{2z} = M_{2x} = M_{2y} = M_{2z} = 0$ for the 3rd link (that is, no force or moment acts at the foot of the spider)

Hence the above matrix for the Link 3 (substituting $\theta = -\theta_3$) simplifies to:

$$\mathcal{T}(-\theta_3) \cdot \mathcal{F}_{1Link\ 3} = \begin{bmatrix} mg\sin(\theta_3) \\ 0 \\ mg\cos(\theta_3) \\ 0 \\ 0 \\ 0 \end{bmatrix} + \begin{bmatrix} m\dot{v}_{Bx} \\ m\dot{v}_{By} \\ m\dot{v}_{Bz} \\ 0 \\ I_{By}\dot{\omega}_{By} \\ I_{Bz}\dot{\omega}_{Bz} \end{bmatrix} + \begin{bmatrix} m\omega_{Bx} \times v_{Bx} \\ m\omega_{By} \times v_{By} \\ m\omega_{Bz} \times v_{Bz} \\ 0 \\ \omega_{By} \times I_{By}\omega_{By} \\ \omega_{Bz} \times I_{Bz}\omega_{Bz} \end{bmatrix}$$

Similarly using $\theta = -\theta_2$ and $\mathcal{F}_{2Link\ 2} = -\mathcal{F}_{1Link\ 3}$ and then $\theta = -\theta_1$ and $\mathcal{F}_{2Link\ 1} = -\mathcal{F}_{1Link\ 2}$, the reactions for link 1 and 2 can be found iteratively. Thus, the moments in each joint of the Spider's leg during a time interval can be found in this manner, when it is in the swing phase and its joint space is known during the time interval.

Least-effort problem for leg in the air (Least-effort Problem 1 or LEP 1):

When one of the legs of the spider is in air, it is basically an open chain manipulator with 4 degrees of freedom, from the 4 revolute joints. If the objective of the leg is to move its foot from one given point to another, there are an infinite number of trajectories that the foot could take. Once the trajectory of the foot is determined, we are still left with one degree of freedom for the 3-link open chain manipulator. Hence there is natural redundancy in the legs of tarantulas. Consequently, some decision making is involved in determining the foot trajectory as well as the last degree of freedom that basically determines the shape of the leg as its foot moves along the trajectory. We use the

least-effort criterion to determine the joint space of the leg when it wants to move from one configuration to another.

Some parameters are already specified for this problem. These are the initial and final positions of the foot, the initial configuration of the leg stated in the joint space and the total time to complete the motion. These parameters come from the final optimization problem described later. It is also worth mentioning that when the leg is swinging, the body may not be still. However, the dynamics of the body are assumed to not affect the leg movement since the body of the spider moves much slower compared to the leg swinging movement. Hence the body is assumed as a fixed ground link in the analysis of the swing phase of the leg.

The foot position is described in 3 dimensions using the polar coordinate system and represented by d , θ_R and ϕ as shown in figure 4 for two different configurations.

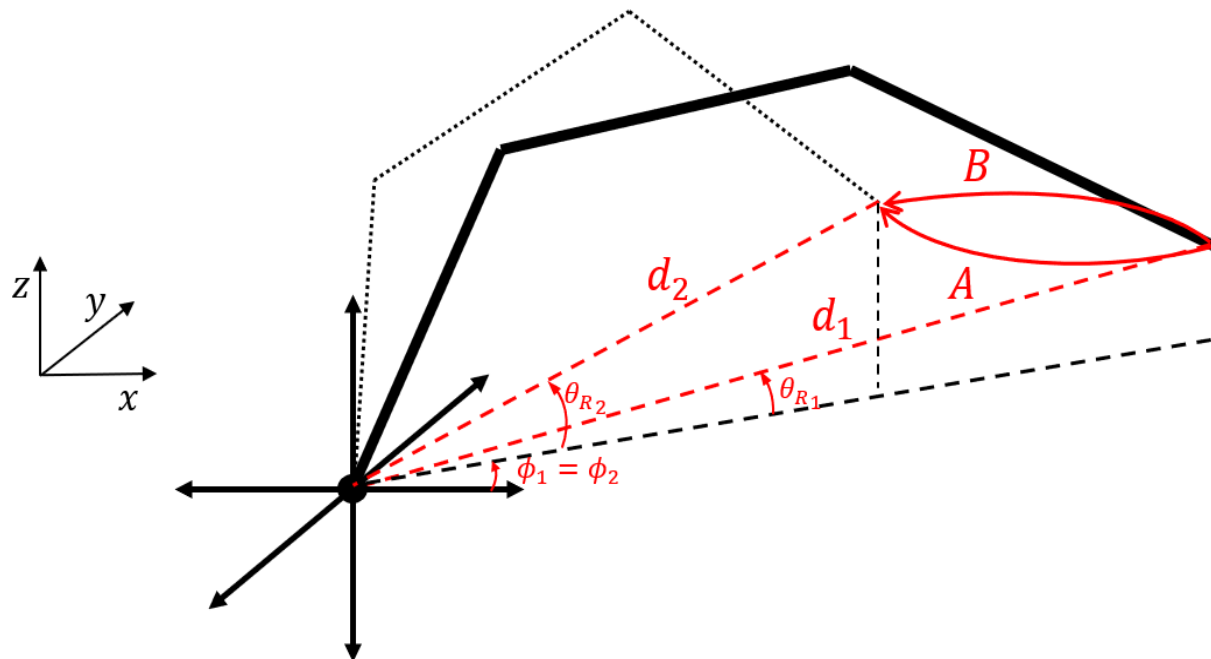


Figure 4: The four parameters used to define the leg configuration in an initial state (solid) and a final state (dotted).

The motion of the foot as it goes from the initial to the final position is defined with respect to time by using a rest-to-rest cubic interpolation of its 3 polar coordinates. Once, the position of the foot with respect to time is defined, another parameter is needed to completely define the leg since it has one redundant degree of freedom. We choose this parameter to be the first joint angle θ_1 and use cubic interpolation to define θ_1 with respect to time. Once θ_1 and the foot position are defined, the remaining joint angles can be determined using trigonometry.

For each cubic interpolation, a scaling parameter ‘ s ’ can be used as follows:

$$s(t) = a_0 + a_1t + a_2t^2 + a_3t^3$$

‘ s ’ is known as the scaling parameter, which is 0 when the leg is at its initial position and 1 when the leg has reached its final position. T is the time taken to go from initial state to final state and T_1 is the time at which a parameters departs from the initial state and T_2 is the time at which is reaches the final state. Each of the four parameters may have a different T_1 and T_2 . Also, for rest-to-rest motions, $s'(t) = 0$ at $t = T_1$ and $t = T_2$. Using these conditions, we get:

$$\begin{aligned} s(t) &= 0 & t \leq T_1 \\ s(t) &= \frac{3 \cdot (t - T_1)^2}{T^2} - \frac{2 \cdot (t - T_1)^3}{T^3} & T_1 < t \leq T_2 \\ s(t) &= 1 & T_2 < t \end{aligned}$$

And,

$$\begin{aligned} d(t) &= d_1 + s_r(t)(d_2 - d_1) \\ \theta_R(t) &= \theta_{R1} + s_{\theta_R}(t)(\theta_{R2} - \theta_{R1}) \\ \phi(t) &= \phi_1 + s_{\phi}(t)(\phi_2 - \phi_1) \\ \theta_1(t) &= \theta_{11} + s_{\theta_1}(t)(\theta_{12} - \theta_{11}) \end{aligned}$$

As mentioned above, a predefined and fixed time interval is allotted to the leg to go from an initial to a final configuration and all the effort expended in the joints of the leg during this interval are considered in the least-effort objective function. We call this time interval, the interval of consideration and denote it by T_{end} . Hence, while T, T_1 and T_2 are defined for each of the 4 parameters, T_{end} is defined for the overall leg motion.

The variables for the optimization problem are chosen as the T_1 and T_2 times of the above parameters. There is a total of 8 of these for the above 4 parameters and they all lie within the interval of consideration with $T_2 > T_1$. The variables are used to derive the joint space of the leg for performing a swing which can then be used to derive the moments in the joints to perform that swing using the matrix equation for the swing phase. The objective function for LEP 1 is defined as the integration of the absolute moments in the 4 joints of the leg over the time interval of consideration. Joint limits are treated as soft constraints and penalized in the objective function.

$$J_{LEP1} = \int_0^{T_{end}} \left(\sum_{n=1}^3 k_n |M_{1y}(t)|_{Link\ n} + k_4 |M_{1z}(t)|_{Link\ 1} + k_5 \cdot JCVP(\phi(t), \theta_1(t), \theta_2(t), \theta_3(t)) \right) dt$$

The first term represents the moments in the revolute joints at endpoint 1 of the 3 links, the second term represents the moment in the revolute joint connecting the leg to body and the JCVP term is the Joint Constraint Violation Penalty term which penalizes the objective function every time the joint constraints are broken. k parameters are used to weigh each term in the objective function depending on joint capabilities.

Physical significance of the variables: Out of the 8 variables, 6 are concerned with the parameters that define the foot position. These variables determine to a degree, the path that the foot will take from initial to final position, since the shortest path for the foot is not necessarily the least-effort

path for the leg. For example, as shown in figure 4, the leg may take path A if T_{1d} and T_{2d} are smaller than $T_{1\theta_R}$ and $T_{2\theta_R}$ respectively (causing the leg to flex first and then rotate), and it may take path B if the opposite was true. The remaining 2 variables are concerned with θ_1 and determine in a way, the shape of the leg or how the leg looks, as it goes from the initial to the final configuration. It is not necessary for any of the variables to coincide with the start or end time of the time interval of consideration. In such cases there are two possibilities, there is either a lag at the beginning of the time interval before the legs starts its motion ($T_1 > 0$) or the leg completes its motion early and then waits at the end position till the time interval of consideration is complete ($T_2 < T_{end}$).

As was discussed above, the foot position at the end and start are known for this problem. In other words, parameters $r_{end}, r_{start}, \theta_{R_{end}}, \theta_{R_{start}}, \phi_{start}, \phi_{end}$ are already known before solving the problem. Also, the leg configuration (All joint angles values of the leg) at the start of the motion is known since this is an initial condition. Hence $\theta_{1_{start}}$ is given already. In some cases, however, the final configuration of the leg and its joints may not be known. In these cases, we let optimization take care of it and $\theta_{1_{end}}$ is also passed as a variable. Thus, the end configuration is left to be determined by least-effort, making the number of variables 9 in all.

Once this problem is solved, we get the configuration of the leg in the joint space with respect to time for least-effort, as it swings from one given position to another. Hence, LEP 1 be used as a subroutine whenever one wants the spider to move its leg for performing higher level motions like walking, jumping, or climbing. Motions that require more than one swings may be divided into phases and LEP 1 can be used to solve for each phase. For example, while walking, a spider first

lifts its leg and then places it on the ground for the next walking cycle. These represent 2 swings, and each swing can be solved individually using LEP 1.

2.5 Leg on the ground phase (The stance phase)

The stance phase of a leg begins as soon as it contacts the ground plane. The leg is then involved in supporting the weight of the spider. A different approach is needed in the analysis of the legs in stance phase since they are not independent of each other.

A standing object needs to contact the ground at 3 points with its center of mass inside the triangle made by the contact points to maintain stability. A spider has 8 legs and each of these undergo a stance phase and a swing phase once during a walk cycle. The stance phase of each leg is longer than the swing phase and hence the spider will always have 4 or more legs in contact with the ground given that it walks symmetrically [24]. Hence its walking motion is over defined at all points of the walk cycle as long as it has its center of mass within the polygon formed by the leg contact points. This redundancy gives a spider much more freedom in deciding when to place a leg and where to place it with respect to the body while walking and we use a least-effort problem to shed light on these decisions. However, before moving to this problem (the final optimization problem), we discuss Least-effort Problems (LEPs) 2 and 3 as its prerequisites.

Least-effort problem for a leg in the stance phase (Least-effort Problem 2 or LEP 2):

The purpose of LEP 2 is to find the best configuration of a stationary leg in the stance phase.

As described before, each leg has 4 degrees of freedom. When the leg is placed on the ground, 3 degrees of freedom are reduced and the last degree of freedom which determines the shape of the leg once its endpoints are fixed is found using least-effort.

The last degree of freedom can be defined by θ_1 (angle between link 1 and horizontal) and we choose this angle as a variable.

For a stationary leg, the velocity and acceleration terms (\mathcal{D}_1 and \mathcal{D}_2) are zero.

A normal reaction force acts at each foot and this force is determined externally (see below).

Moreover, a horizontal force resulting from the friction and adhesive forces acting at the spider's foot is assumed to be acting in the leg plane and pointing radially inwards. We call this force as the ground plane force.

Hence the link matrix equation for the 3rd link simplifies to:

$$\mathcal{J}(-\theta_3)\mathcal{F}_{1link\ 3} = \begin{bmatrix} F_H \cos(\theta_3) - F_N \sin(\theta_3) \\ 0 \\ -F_N \cos(\theta_3) - F_H \sin(\theta_3) \\ 0.5F_H l \sin(\theta_3) + 0.5F_N l \cos(\theta_3) \\ 0 \\ 0 \end{bmatrix} + \begin{bmatrix} mg \sin(\theta_3) \\ 0 \\ mg \cos(\theta_3) \\ 0 \\ 0 \\ 0 \end{bmatrix}$$

Where F_H and F_N are the ground plane and normal forces acting on the foot.

Similarly using $\theta = -\theta_2$ and $\mathcal{F}_{2Link\ 2} = -\mathcal{F}_{1Link\ 3}$ and then $\theta = -\theta_1$ and $\mathcal{F}_{2Link\ 1} = -\mathcal{F}_{1Link\ 2}$, the reactions for link 1 and 2 can be found iteratively. Thus, the moments in each joint of the spider's leg can be found when it is in the stance phase. The objective function is simply the sum of absolute values of the moments.

$$J_{LEP2} = \sum_{n=1}^3 |M_{1y}|_{link\ n}$$

The revolute joint connecting the leg to the body is not involved here since the leg is static.

The inputs for LEP 2 are the location of the two end points of the leg (The body and the foot) and the forces acting at the foot of the body. (Normal and ground plane forces)

2.6 Calculating the normal forces:

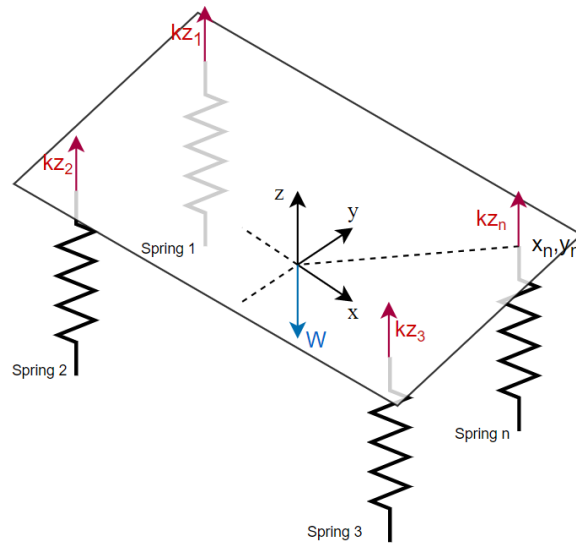


Figure 5: Equivalent spring mass system of the spider with n legs in contact with the ground.

The normal forces acting on the foot of each leg of the spider when it stands, or walks depend on the number of legs in contact with the ground at once and the distance of each foot from the center of mass of the spider.

Since this system is usually statically indeterminate (More than 3 legs are in contact with the ground at once), it is solved by treating it as an equivalent spring mass system where the entire spider is treated as a mass supported by legs which are treated as springs with unit spring constant ($k = 1$). To balance the moments about the horizontal directions, the spring farthest from the center of mass displaces the least while the nearer ones impart more force and accordingly displace more. This equivalently results in a reduced normal force in a leg as the distance between the foot and the center of mass increases. This is described using equations as follows:

Let the number of legs in contact with ground be n , where:

$$3 \leq n \leq 8$$

Then the deformation in each spring is the superposition of the longitudinal deformation along the z axis, z_w and the angular deformations about x and y axis α and γ . z_i is the deformation in the i th spring and W is the total weight of the spider. We have,

$$z_1 = z_w + \tan(\alpha)(y_1) - \tan(\gamma)(x_1)$$

$$z_2 = z_w + \tan(\alpha)(y_2) - \tan(\gamma)(x_2)$$

$$z_3 = z_w + \tan(\alpha)(y_3) - \tan(\gamma)(x_3)$$

$$z_n = z_w + \tan(\alpha)(y_n) - \tan(\gamma)(x_n)$$

Force Balance:
$$z_1 + z_2 + z_3 + \dots + z_n = -\frac{W}{k} = -W$$

Moment balance about x :

$$-y_1 z_1 - y_2 z_2 - y_3 z_3 - \dots - y_n z_n = 0$$

Moment balance about y :

$$x_1 z_1 + x_2 z_2 + x_3 z_3 + \dots + x_n z_n = 0$$

Hence:

$$\begin{aligned} n z_w + \tan(\alpha) \left(\sum_{i=1}^n y_i \right) - \tan(\gamma) \left(\sum_{i=1}^n x_i \right) &= -W \\ - \left(\sum_{i=1}^n y_i \right) z_w - \sum_{i=1}^n y_i^2 \tan(\alpha) + \sum_{i=1}^n x_i y_i \tan(\gamma) &= 0 \\ + \left(\sum_{i=1}^n x_i \right) z_w + \sum_{i=1}^n x_i y_i \tan(\alpha) - \sum_{i=1}^n x_i^2 \tan(\gamma) &= 0 \end{aligned}$$

$$\begin{bmatrix} n & \sum y_i & -\sum x_i \\ -\sum y_i & -\sum y_i^2 & \sum x_i y_i \\ \sum x_i & \sum x_i y_i & -\sum x_i^2 \end{bmatrix} \begin{bmatrix} z_w \\ \tan(\alpha) \\ \tan(\gamma) \end{bmatrix} = \begin{bmatrix} -W \\ 0 \\ 0 \end{bmatrix}$$

After solving the above matrix and substituting the derived values to find z_i , we get the normal force acting on the i th foot.

2.7 Calculating the ground plane forces (Least-effort Problem 3 or LEP 3):

When the spider is standing, the ground plane forces at its feet alleviate the joint effort it must exert to keep standing. We calculate these ground plane forces for a standing spider next for any number of legs between 3 and 8 in contact with the ground using LEP 3.

As stated before, all ground plane forces are assumed to point radially inwards (that is, they lie in the leg plane of each leg). To understand the reasoning and intuition for this, one can imagine standing on their 4 limbs together. When the contact points are far enough for slipping to begin, the feet (and hands) tend to slip approximately radially and before slipping occurs, friction tends to prevent leg extension and slipping along this direction. Hence the direction of the ground plane forces can be approximated to point radially inward, and the only unknown is its magnitude. For a given set of feet positions, the normal forces are first calculated at each foot as described above. An optimization problem is then formulated with n variables for n ground plane forces, one for each of the n legs in the stance phase. Here,

$$3 \leq n \leq 8$$

The resultant of these forces is zero in the ground plane and hence the variables are subject to 2 constraints. The constraints are described as follows:

$$F_{H_1} \cos(\phi_1) + F_{H_2} \cos(\phi_2) + F_{H_3} \cos(\phi_3) + \dots + F_{H_n} \cos(\phi_n) = 0$$

$$F_{H_1} \sin(\phi_1) + F_{H_2} \sin(\phi_2) + F_{H_3} \sin(\phi_3) + \dots + F_{H_n} \sin(\phi_n) = 0$$

Where, ϕ_n is the leg plane angle of the n^{th} leg. For each run of the optimization, the leg configuration of each leg in stance phase is calculated from LEP 2. The objective function is the sum of absolute value of the constant moments generated from standing while the set of n ground plane forces act on the feet of the spider. These moments can be calculated from the stance phase matrix formulation defined in section 2.5.

$$J_{LEP3} = \sum_{i=1}^n \sum_{j=1}^3 |M_{1y}|_{link\ j\ of\ leg\ i}$$

Thus, the set of n forces that generate least moments in the joints is selected.

2.8 The Final Optimization Problem

The FOP is used to derive complete walking gaits for the spider and all associated joint angles as it walks on a flat horizontal surface. Walking of all animals is cyclic in nature and is performed by repeating the same motions after each stride. Hence in our problem, we consider only a single stride, and all associated joint moments exerted while performing this stride. We call this interval, the walking gait cycle due to its cyclic nature.

For every complex system, a few assumptions are required to simplify the problem. One of the important assumptions we make to simplify our problem formulation is symmetrical walking about the sagittal plane. Thus, every motion performed by the legs on the right side of the spider will also be performed by the corresponding legs on the left side of the spider after half time of the walking gait cycle. This reduces the number of variables by half and aids in a much easier and accurate analysis. The duty factors for each leg (The fraction of the walking gait cycle for which

the leg is in the stance phase) are stated beforehand using information from previous studies in biomechanics [22],[24],[27],[28]. All swing phase motions performed during the walking gait cycle are calculated independently from the remainder of the spider using LEP 1 and a leg that is in the swing phase is assumed to not affect the rest of the spider since it is much lighter in weight.

Another important assumption is that of the quasi-static walking condition of the spider. Under normal conditions, a tarantula moves relatively slowly except for when it is in danger or in a state of urgency especially while hunting [25]. Our studies showed us that when in support phase, the static forces dominated the dynamic forces by a factor of 10 and accordingly, a tarantula spends much more effort in standing than in propelling itself to walk. For this reason, we treat the stance phase as a quasi-static problem because this allows for a more rigorous yet simpler analysis of the walking gaits. When a leg is in the support phase, the dynamic forces it produces at its feet for

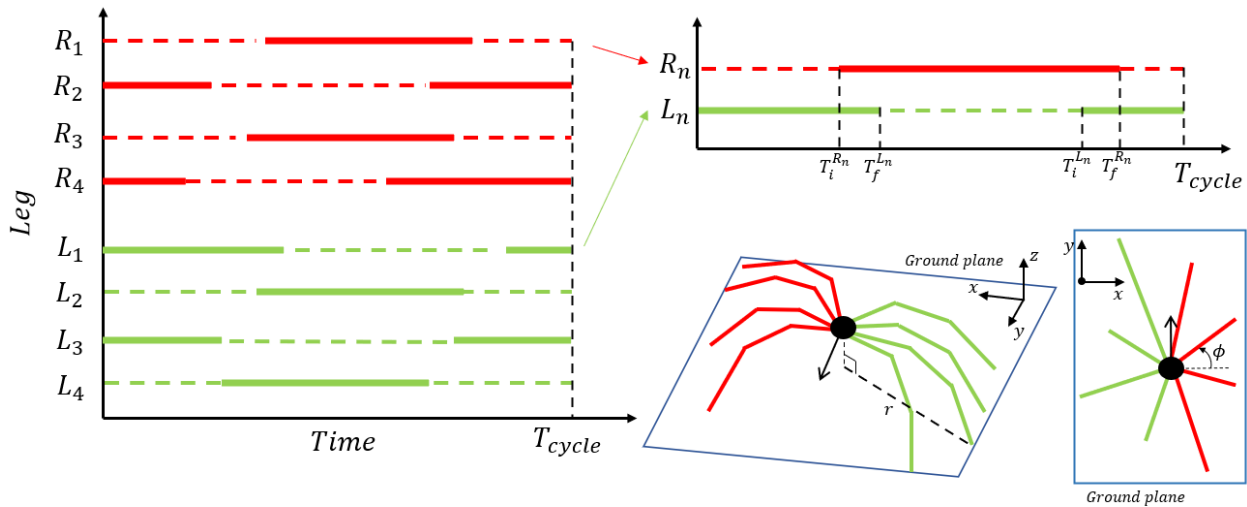


Figure 6: Illustration of various notable parameters used in the FOP. A sample gait phase diagram (left) is shown for the spider. Gait phase diagrams on top right illustrate the times when the phase of a leg is flipped from the stance or swing phase. Figures at the bottom right illustrate the leg radius (r) and the leg plane angle (ϕ).

pushing and steering the body are neglected. Each position that the spider passes through to perform the walking motion (hence the quasi) is treated as if the spider was standing in that position

(hence the static) and the effort in the joints for all these stances are integrated over time giving the complete effort expense for the walking gait cycle.

The FOP comprises of 12 variables. Each of the 12 variables are described in further detail below.

Description of variables (refer to Figure 6):

As shown in the figure, each leg has a single T_i time (when the leg is placed on the ground) and a single T_f time (when the leg is lifted from the ground) per walking gait cycle. A leg may contact the ground in one cycle and break contact in the next cycle (resulting in T_i falling after T_f for that leg in the walking gait cycle).

The first 4 variables are selected as the T_i times of the 4 right legs of the spider. The T_i times of the 4 legs on the left are determined using left-right symmetry while walking with the help of the following equations:

$$T_i^{Ln} = T_i^{Rn} + T_{cycle}/2$$

Where L and R denote Left and Right respectively and $n = 1, 2, 3, 4$ for the four legs on each side. T_{cycle} is the total time of the walking gait cycle.

The T_f times of each leg are determined using the equations:

$$T_f^{Rn} = T_i^{Rn} + T_{DF}^{Rn}$$

$$T_f^{Ln} = T_i^{Ln} + T_{DF}^{Ln}$$

Where DF stands for Duty Factor and T_{DF} the time for which a leg is in the stance phase.

The next 4 variables influence how far a leg is placed from the body while walking. As seen in the figure, r or the leg radius is defined as the component of the distance along the ground plane

between the foot of a leg and the body. The next 4 variables are selected as the values of r for the 4 right legs, when they contact the ground (that is, at time $t = T_i^{Rn}$). They are denoted by r^{Rn} and n denotes the n th leg. Note that r^{Rn} at T_i^{Rn} is equal to r^{Ln} at T_i^{Ln} (Due to symmetry).

The last 4 variables influence the direction of the legs as the spider walks. The leg plane angle of the n^{th} leg on the right is given by ϕ^{Rn} . The last 4 variables are selected as the values of ϕ of each of these 4 legs, when they contact the ground (that is, at time $t = T_i^{Rn}$). Note that ϕ^{Rn} at T_i^{Rn} is equal to ϕ^{Ln} at T_i^{Ln} (Due to symmetry).

Table 3: List of all parameters used in the FOP.

Parameter	Equivalent to	Description
T_i^{Rn}	Variables 1-4 for $n = 1, 2, 3, 4$	Time instant in the walking gait cycle at which the n^{th} leg on the right contacts the ground
T_i^{Ln}	$T_i^{Rn} + T_{cycle}/2$	Time instant in the walking gait cycle at which the n^{th} leg on the left contacts the ground
T_f^{Rn}	$T_i^{Rn} + T_{DF}^{Rn}$	Time instant in the walking gait cycle at which n^{th} leg on the right enters the swing phase
T_f^{Ln}	$T_i^{Ln} + T_{DF}^{Ln}$	Time instant in the walking gait cycle at which n^{th} leg on the left enters the swing phase
r^{Rn} (At T_i^{Rn})	Variables 5-8 for $n = 1, 2, 3, 4$	Component of distance along the ground plane between the body and the foot of the n^{th} leg on the right when it contacts ground
r^{Ln} (At T_i^{Ln})	r^{Rn} (At T_i^{Rn}), Variables 5-8	Component of distance along the ground plane between the body and the foot of the n^{th} leg on the left when it contacts ground
ϕ^{Rn} (At T_i^{Rn})	Variables 9-12 for $n = 1, 2, 3, 4$	Leg plane angle of the n^{th} leg on right when it contacts the ground
ϕ^{Ln} (At T_i^{Ln})	ϕ^{Rn} (At T_i^{Rn}), Variables 9-12	Leg plane angle of the n^{th} leg on left when it contacts the ground

All parameters and variables related to the walking gait cycle are summarized in table 3.

Deriving the objective function value for the FOP is a procedure explained using a flowchart shown in figure 7. As described in the flowchart, the variables from an optimization run and the physical parameters of the spider such as mass, link lengths, duty factors of each leg are needed to initiate the calculation of the objective function. Once these are supplied, the next thing that is done is finding the stance and swing phases of each leg. This is done using the first 4 time variables and the duty factors of each leg. Each time step of the walking gait cycle can be classified as a stance phase or a swing phase for each leg. A leg would change its state exactly twice during one cycle. For a given stride length, velocity and body height, the body position at each time instant is calculated next. The body moves in a straight line along the direction of the given velocity at a fixed height. The velocity of the body is modelled as sinusoidal with 2 crests and 2 troughs per walking gait cycle [28]. Using the body and foot positions (determined by 8 of the variables) the values of r or the leg radius and ϕ or the leg plane angle can be found during the stance phases for each leg. Since the foot positions are known at this point, the normal forces at each leg can be found using the equivalent spring-mass system in section 2.6.

The leg configurations in the stance phase are then calculated using LEP 2. However, it must be noted that the ground plane forces which come from LEP 3 and are needed for LEP 2 are not known at this point, since it is necessary to define the complete joint space to solve LEP 3. To resolve this, we supply the ground plane force as a variable to LEP 2. This is done because the ground plane forces are also supplied as a variable to LEP 3 and both the LEPs have the same objective of minimizing the joint efforts. The difference is that the ground plane forces coming from all the legs are coupled in LEP 3 through 2 constraints that ensure that their resultant is 0.

These constraints may obscure the ground plane forces from what they would have been if each leg was treated independently (as in LEP 2). However, our studies have shown that the optimal leg configuration remains the same for a large range of ground plane force values. We call this leg configuration as the θ_{1max} configuration and it is discussed in further detail in the results section. This particular optimal configuration has a wide low effort region and is discussed later in the results section.

Once the leg configurations are completely defined in the joint space, the actual, coupled ground force values can be found from LEP 3. At the same time, all the swing phase motions of each leg during the walking gait cycle are found using LEP 1. The final and initial leg configurations of the stance phase become the initial and final leg configurations respectively of the swing phase.

Now that the leg configurations and all the external forces are known, the effort in the joints can be evaluated from the matrix equation of each of the 24 links. The effort cost for the entire spider during the walking gait cycle can then be calculated as follows:

Total effort in the walking gait cycle:

$$J_{FOP} = k_6 \cdot (\Delta LED) + \int_0^{T_{cycle}} \left(\sum_{i=1}^8 \left(\sum_{j=1}^3 k_j |M_{1y}(t)|_{Link j} + k_4 |M_{1z}(t)|_{Link 1} \right)_{Leg i} + k_5 \cdot JCVP(\phi_i(t)) \right) dt$$

ΔLED is the Leg Effort Difference term representing the total of the difference between the effort values of each leg. It is included to ensure that all legs contribute a similar amount of effort, and a few legs are not taking much higher load than the rest.

$JCVP$ is the Joint Constraint Violation Penalty that ensures that the feet of all legs are within their range and that the legs do not collide with each other. Thus, this procedure gives the best set of 12 variables that minimize and equalize the effort in the spiders legs while walking. These 12 variables are used to reconstruct the walking gait for the spider walking on a flat surface. To make

the spider walk along a different direction, we simply turn the frame of reference and align it with the direction in which the spider is walking.

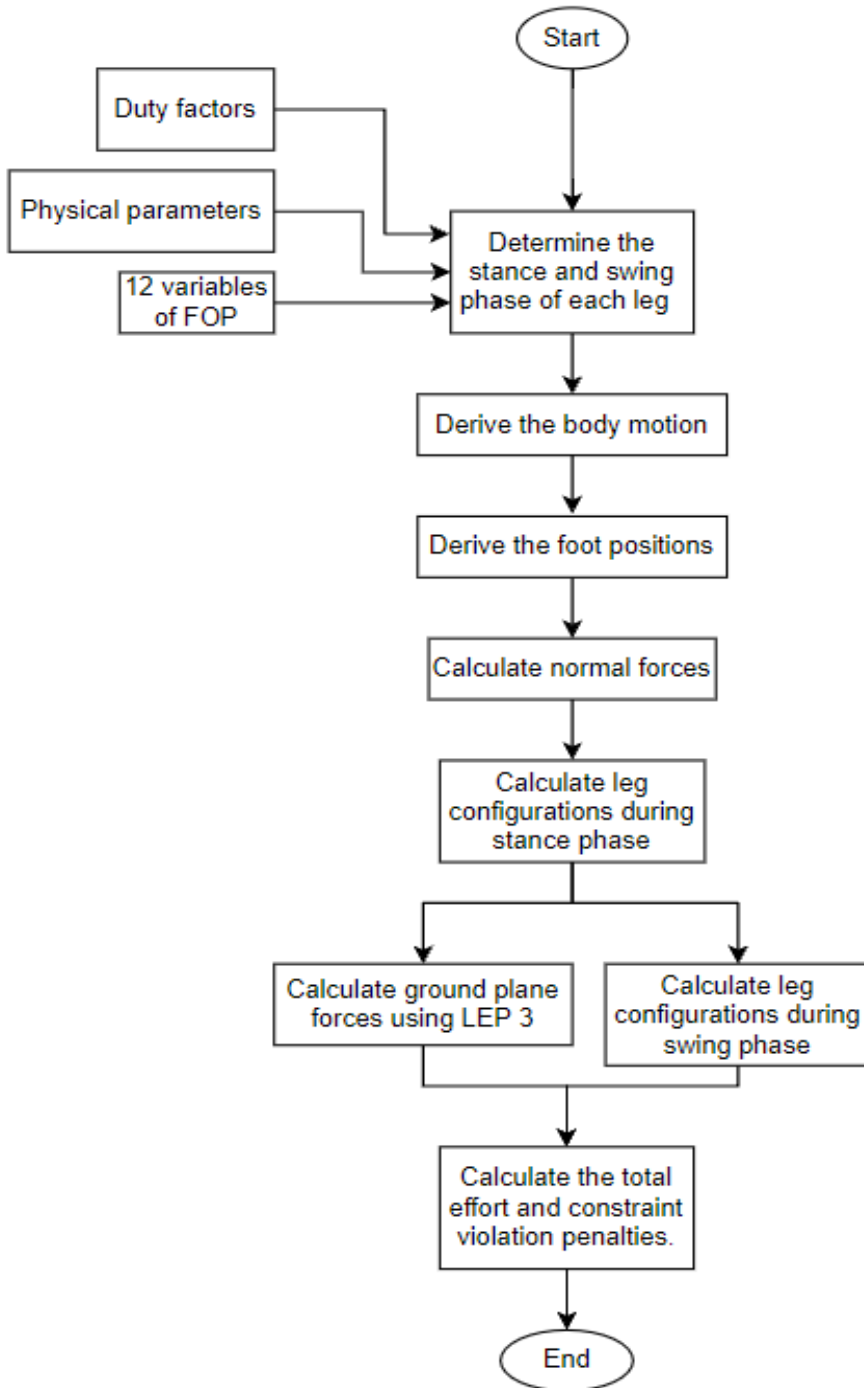


Figure 7: Flowchart of the complete procedure of calculating the objective function for the FOP.

3. Results

In this section we shed light upon the various motions performed by the tarantula spider while walking as derived by our hierarchical procedure of optimization. Since each least-effort problem holds some physical significance, we discuss the results of each LEP separately, followed by a discussion about the final walking gaits obtained from FOP.

3.1 Least-effort Problem 1 Results:

As discussed above, LEP 1 gives the configurations of a leg in the joint space as it swings its foot from one position to another. The swinging motion of a particular leg is treated independently from the rest of the body and legs. LEP 1 is expected to provide fluid, natural swing phase motions similar to the ones performed by a tarantula. To find the degree of resemblance in the derived motions, we compare them in figure 8 with a single swing of a tarantula. The first series of images, the '*a*' series are screenshots taken from a YouTube video of a tarantula walking on a flat surface [29]. The second series or the *L* series is that obtained from least-effort while the 3rd series or the *s* series show the motion performed when the foot takes the shortest direct path from the initial to final position. All the screenshots are taken at uniform, equally distributed intervals of time in each series. The motion demonstrated in the figure is a common reaching out motion performed by the forelegs of the tarantula while walking. The path traced by the foot in each case is shown by red.

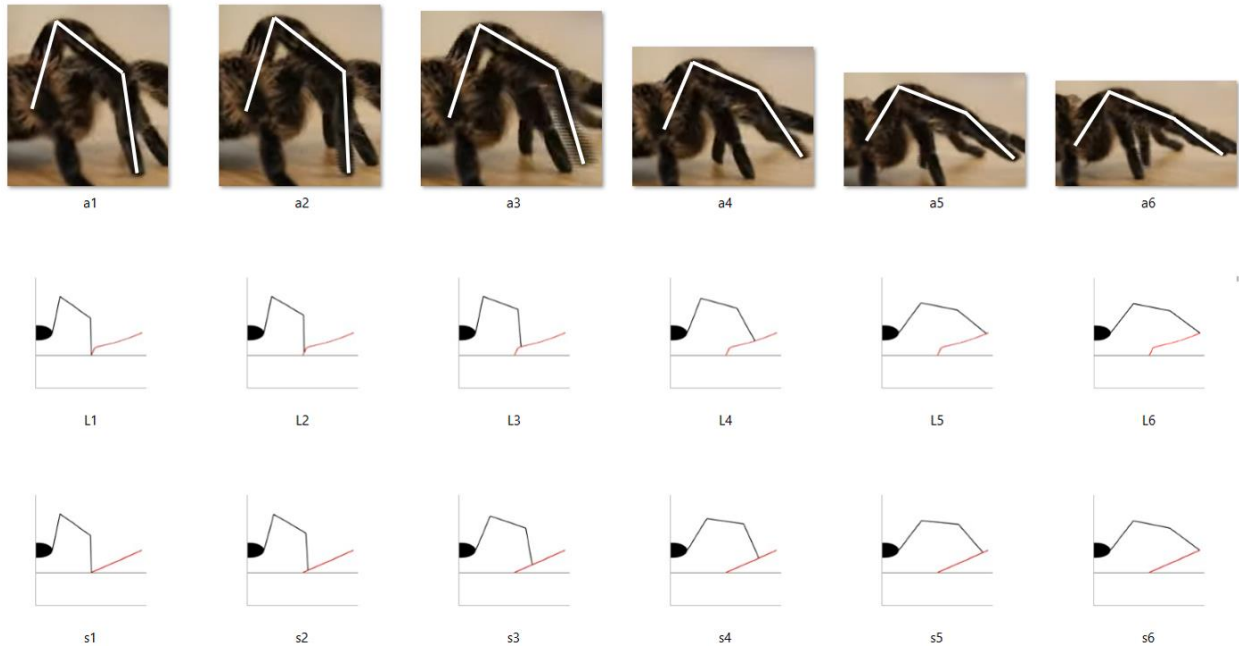


Figure 8: Series of images showing a leg flexing for same initial and final conditions. The 'a' series was taken from an online video of a spider. The 'L' series show the motion derived using least effort principle. For the 's' series, the foot follows a straight-line path from initial to final position. White lines overlapping with the leg links are drawn for the first series for easier comparison.

From the figure, it is clear that the least-effort or the *L* series tends to keep the leg closer to the body for a longer time before extending it (see link 1 in *L* series). Overall, the *L* series matches well with the actual motion of the tarantula. The *s* series wherein the foot follows a straight line tends to form a trapezium like shape due to early withdrawal of the first link whereas the *L* series tends to lift the leg first and then extend it outwards.

3.2 Least-effort Problem 2 and 3 Results:

Least-effort problems 2 and 3 have more to do with how the legs behave when they are in contact with the ground and are supporting the body as the spider walks. As stated before, even though dynamics are considered for when the leg is swinging, the spider as a whole is treated as a quasi-static system and each time step of the walking gait cycle can be treated as if the spider was standing in that position at that time step. Hence, LEP 2 and LEP 3 are static problems used for the stance phase to find best case scenarios for when the spider is in a fixed position.

For LEP 2 which gives the leg configuration that produces minimum effort in the joints for a given foot position and set of foot forces (normal force and ground plane force), it is observed that the spider tends to keep the first link as close to the body as possible. This may be done to keep the leg mass close to the body. Since the first joint is physically constrained to be below 90° , the first joint angle as derived by LEP 2 is at its physical constraint limit of 90° (refer table 2) when the foot is closer to the body while it is at its geometric limit (causing links 2 and 3 to form a straight line as shown in figure) when the foot is farther from the body (See Fig. 9). This configuration can be called as the $\theta_{1,max}$ configuration and it is the optimal configuration for a wide range of ground plane forces applied at the foot. Figure 10 shows 2 curves for the two cases of foot-positions shown in Figure 9. These curves represent the optimal θ_1 (represented by θ_1^*) and the associated cost value from LEP 2, plotted against various values of ground plane forces ranging from 0 to 40% of

the spider's total weight. The normal force applied at the foot is constant 0.25 times body weight for both cases. It is apparent that the $\theta_{1_{max}}$ leg configuration (which is 90° or the geometric limit,

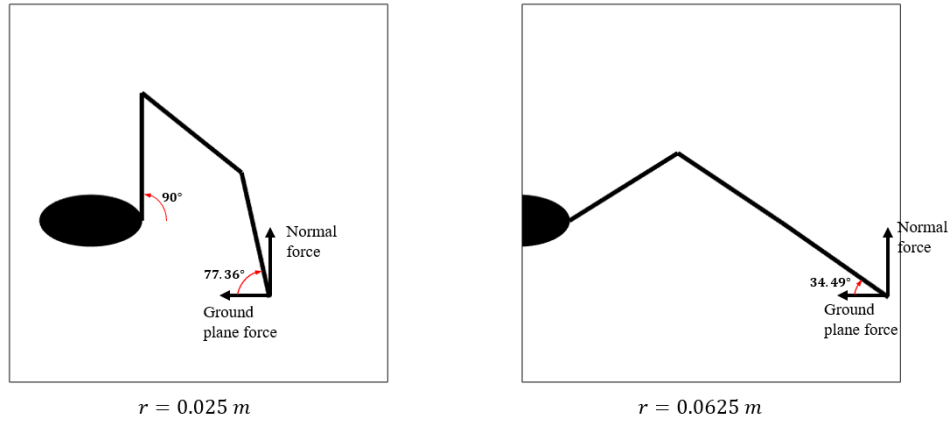


Figure 9: Least effort leg configurations derived from LEP 2 shown for two locations of the foot. The foot is nearer to the body resulting in a smaller foot radius and $\theta_{1_{max}} = 90^\circ$ while the leg is stretched out in the 2nd case resulting in a large foot radius and $\theta_{1_{max}}$ is at its geometric limit.

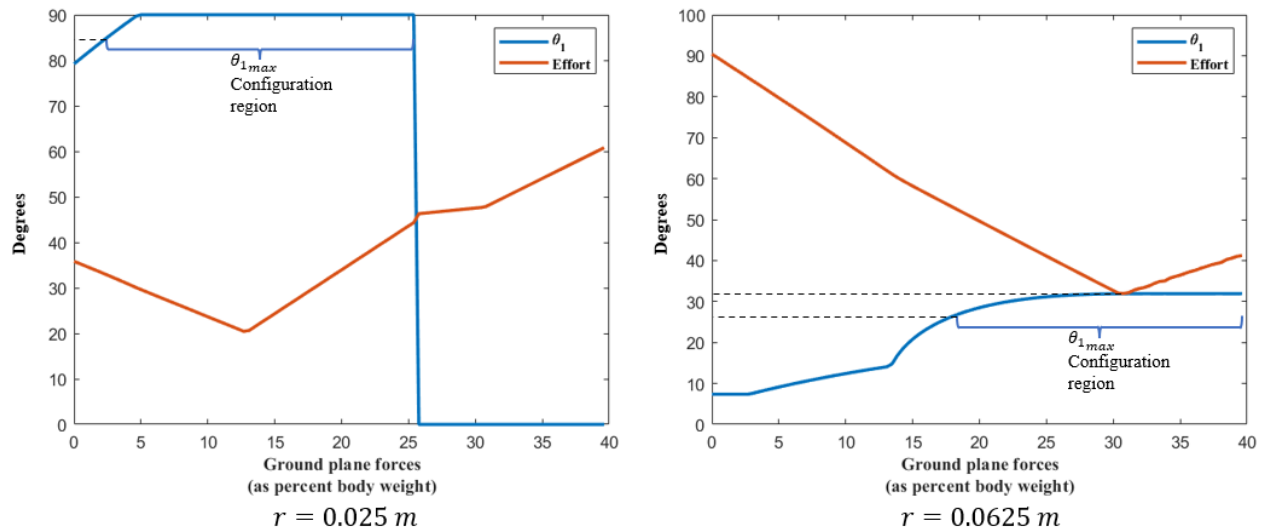


Figure 10: The $\theta_{1_{max}}$ configuration region is illustrated for two-foot positions and the associated effort variation with the ground plane forces is shown for each case. Effort has been scaled to fit the same window as θ_1 .

whichever is smaller) holds true for a wide range of ground plane forces. Let this region be called the $\theta_{1_{max}}$ configurations region and we define it as the range of ground plane forces where θ_1^*

does not change by more than 5° from θ_{1max} . The θ_{1max} configurations region for the 2 cases are shown in the plots. This result proves useful when evaluating the objective function for FOP where the ground plane forces need to be approximated in LEP 2 to find the leg configuration, since they come from LEP 3 which cannot be solved without solving LEP 2 first. Hence the plots reveal that even with approximations for ground plane forces, the θ_{1max} leg configurations derived from LEP 2 may be near optimum configurations for the ground plane forces derived from LEP 3.

Another notable observation is the angle made with the ground plane by the 3rd link when the foot is far from the body (2nd case in Fig. 9). This is a common case for the anterior legs of the spider that need to stretch out before entering the stance phase for pulling the body forward while walking. Studies have shown that as the anterior legs stretch out in the air, they approach the ground with a 30° angle. This might have to do with minimizing joint efforts of the leg for its upcoming stance phase. With a spider having to extend its anterior legs by over two link lengths while walking, the θ_{1max} leg configuration as derived by LEP 2 results in an approach angle of about 30° as shown in figure 9.

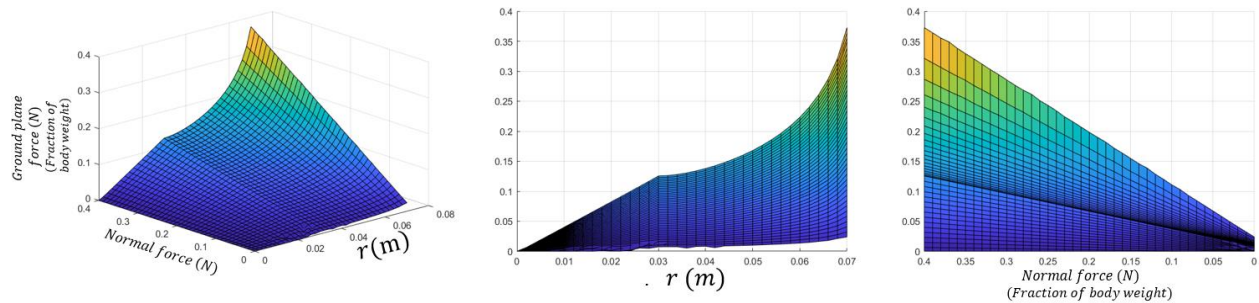


Figure 11: Variation of the optimal ground plane force with Leg radius and Normal force. The ground plane force for a leg increases with an increase in normal force and leg radius.

Moving on, we have LEP 3 that is concerned with finding the best set of ground plane forces acting at the feet of the legs in the stance phase. Figure 11 shows the dependence of the ground plane force on the leg radius r as well as normal forces acting at the foot. In all cases the leg configuration is the $\theta_{1,max}$ configuration. The ground plane forces increase linearly with the normal force since this means that the weight load of the body on this leg is increasing.

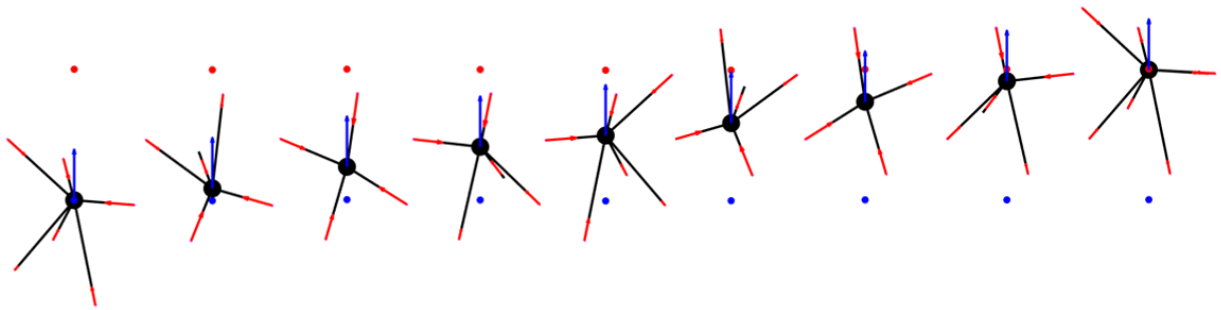


Figure 12: Demonstration of optimal ground plane forces derived from LEP 3 using red arrows as the body moves from the blue dot to the red dot. Larger arrows represent a larger force. The blue arrow represents walking direction.

The relation with foot radius is linearly increasing till a foot radius of 0.03 and this relation becomes exponential with further increase in radius. When the foot radius is 0.03, the leg configuration crosses its zone of physical constraint limit for θ_1 and enters the geometric limit zone. In other words, θ_1^* is 90° till this point and reduces according to the geometric limit as the foot radius increases over 0.03. However, these relations do not always hold true, since the ground plane forces are constrained by two equations that bring about their resultant in the ground plane to be zero. The progression of ground plane forces for a alternating tetrapodal walking gait as derived by LEP 3 is shown in figure 12. The LEP 3 is solved for each time step of the walking gait cycle.

3.3 The Final Optimization Problem Results:

This section lays out results for the final optimization problem that is concerned with holistically deriving the overall walking motion and the decisions taken while walking, such as which legs to use and when to use them during a walking gait cycle and also, how these legs should be placed. The problem also makes use of LEP 1,2 to determine movements within each leg as they are extended and retracted while walking and LEP 3 to determine the ground plane forces at the feet at each time step of the walking gait cycle.

Some of the important results of this problem are the group of legs used at a time (an important factor in determining the walking gait of the spider), and the overall foot placement location. Abnormal foot placements may lead to a high amount of unbalance as the spider walks leading to tremendous effort in the joints of certain legs. The weight of the spider should be well distributed, and the gait should allow the spider to use each of its legs uniformly to allow for a smooth and fluid walking motion. Also, using a specific group of legs at a time would lead to better balancing and weight distribution. For example, using all the legs on the left side at one time and then the ones on the right side next (similar to how a human walks) would be difficult to do for a spider since its body weight is not directly above its feet and would result in tremendous efforts in the joints. Research has repeatedly shown [22],[23],[24],[27],[28] that a spider's walking gait approximately involves an alternating tetrapodal gait where in four alternate legs (such as R1, L2, R3, L4) do the work for one half of the walking gait cycle and the next four alternate legs (L1, R2, L3, R4) work for the next half. These are some of the results we look forward to deriving through least-effort in this subsection.

As stated before, this optimization problem comprises of 12 variables, first 4 of which determine when the legs establish contact with the ground and next 8 determine where the legs are placed during the walking gait cycle. Tables 4 and 5 show the optimization results for the FOP. A total of 45 Optimizations were carried out using the genetic algorithm for two stride lengths: 0.035 m and 0.038 m. Evidently, GA did not always converge to the same set of optimal variables. Firstly, due to the symmetry assumption, two sets of optimal variables may have identical solutions for the 8 leg placement variables while the four time variables in the sets may be offset by $T_{cycle}/2$. Thus, the movement produced by the first set would be a left-right mirror image of that produced by the second. Secondly, since the objective function is not perfect but involves a number of assumptions and approximations, GA may find other solutions that have a low cost for our objective function but in reality, consume more effort. Furthermore, for the same reason, we treat a range of objective costs as acceptable instead of just picking the one with the lowest cost.

The alternating-tetrapodal gait patterns that exist in nature were also some of the solutions found by the GA and they are marked in green. Out of 45 runs, GA converged to the expected alternating-leg gait pattern in 21 runs where 9 were found for the 0.035m stride length and 12 for the 0.038m stride length. Out of all the green runs, run #15 has been selected for further discussion, since this best matched what we observe in tarantulas while also having a comparatively low objective cost.

Table 4: Optimization results for stride length of 0.035m.

Run	Foot Location Variables								Time Variables in sec				Obj cost
	Leg Radius (r) in cm				Leg Plane Angle (ϕ) in rad								
1	5.82	4.53	2.27	1.45	1.258	0.785	-0.037	-0.806	0.50	0.04	0.41	0.33	5855
2	5.74	4.96	3.32	1.62	1.447	0.785	0.000	-0.785	0.06	0.42	0.02	0.30	5791
3	5.77	4.97	3.14	1.41	1.198	0.785	0.000	-0.792	0.03	0.29	0.69	0.26	5609
4	5.74	4.58	3.08	1.34	1.315	0.785	-0.082	-0.785	0.47	0.04	0.44	0.72	5841
5	5.85	4.53	2.28	1.44	1.238	0.785	-0.090	-0.788	0.46	0.74	0.34	0.28	5596
6	5.85	4.23	2.07	1.39	1.230	0.785	-0.052	-0.785	0.42	0.75	0.31	0.27	5569
7	5.83	4.24	3.00	1.55	1.554	0.785	-0.170	-0.785	0.51	0.25	0.65	0.76	5907
8	5.88	4.94	3.51	1.34	1.464	0.785	0.000	-0.785	0.08	0.51	0.11	0.33	5826
9	5.85	4.92	2.88	1.70	1.269	0.785	-0.009	-0.785	0.50	0.67	0.27	0.35	5566
10	5.78	4.94	3.15	1.42	1.209	0.785	0.000	-0.787	0.80	0.28	0.68	0.25	5623
11	5.89	4.91	2.97	1.58	1.291	0.781	-0.014	-0.786	0.54	0.72	0.32	0.39	5778
12	5.82	5.48	2.24	1.76	1.566	0.785	-0.004	-0.800	0.44	0.19	0.62	0.69	5943
13	5.73	4.96	3.30	1.60	1.452	0.785	0.000	-0.785	0.44	0.79	0.39	0.68	5763
14	5.90	4.25	2.11	1.39	1.251	0.785	-0.149	-0.785	0.42	0.73	0.32	0.27	5552
15	5.650	5.040	3.200	1.610	1.470	0.785	0.000	-0.785	0.42	0.75	0.36	0.67	5752
16	6.21	5.35	2.93	1.51	1.324	0.785	-0.001	-0.797	0.49	0.66	0.26	0.34	5779
17	5.59	5.47	2.64	1.57	1.265	0.785	0.000	-0.805	0.54	0.69	0.34	0.39	5777
18	5.76	4.08	2.59	1.59	1.569	0.778	-0.290	-0.791	0.42	0.28	0.71	0.64	5818
19	5.49	4.85	3.25	1.49	1.491	0.785	-0.001	-0.853	0.12	0.45	0.04	0.70	5935
20	5.88	4.98	3.59	1.34	1.473	0.785	0.000	-0.785	0.08	0.52	0.12	0.33	5824
21	5.77	5.11	2.86	1.74	1.275	0.785	-0.022	-0.785	0.51	0.67	0.29	0.36	5618
22	5.64	5.39	2.52	1.64	1.272	0.785	0.000	-0.876	0.52	0.68	0.32	0.37	5687
23	5.98	4.42	2.37	1.43	1.299	0.785	-0.104	-0.791	0.80	0.27	0.67	0.65	5517

Table 5: Optimization results for stride length of 0.038m

Run	Foot Location Variables								Time Variables in sec				Obj cost
	Leg Radius (r) in cm				Leg Plane Angle (ϕ) in rad								
24	5.93	5.38	3.37	1.67	1.429	0.784	0.000	-0.785	0.77	0.28	0.68	0.21	5946
25	6.23	5.48	3.55	1.69	1.470	0.783	-0.001	-0.791	0.06	0.36	0.01	0.29	6031
26	6.23	4.72	3.15	1.89	1.368	0.782	-0.016	-0.789	0.76	0.27	0.68	0.21	6033
27	6.23	4.79	2.89	1.57	1.306	0.785	-0.015	-0.787	0.80	0.24	0.61	0.64	5964
28	6.28	5.73	2.77	1.68	1.304	0.785	-0.003	-0.786	0.79	0.24	0.61	0.64	5832
29	6.03	5.38	3.37	1.67	1.353	0.785	0.000	-0.786	0.07	0.23	0.65	0.70	5838
30	6.03	5.48	3.35	1.69	1.417	0.784	0.000	-0.786	0.77	0.28	0.68	0.21	5956
31	6.31	4.73	3.37	1.63	1.425	0.784	0.000	-0.786	0.77	0.28	0.68	0.21	5970
32	5.90	5.39	3.35	1.61	1.447	0.785	-0.010	-0.785	0.44	0.11	0.46	0.69	6077
33	6.23	5.48	3.55	1.69	1.442	0.785	0.000	-0.785	0.77	0.28	0.68	0.22	5927
34	6.12	4.17	2.13	1.56	1.384	0.782	0.000	-0.786	0.76	0.27	0.68	0.21	6028
35	6.26	4.69	2.29	1.57	1.259	0.785	-0.026	-0.785	0.79	0.33	0.66	0.64	5784
36	6.21	5.35	2.93	1.51	1.266	0.785	-0.101	-0.785	0.08	0.43	0.00	0.70	6069
37	6.04	5.54	3.36	1.55	1.324	0.785	-0.001	-0.797	0.49	0.66	0.26	0.34	5779
38	5.90	5.40	3.37	1.61	1.571	0.785	-0.049	-0.816	0.05	0.75	0.40	0.68	6040
39	6.37	5.26	3.59	1.93	1.440	0.785	0.000	-0.785	0.77	0.28	0.68	0.22	5928
40	6.22	5.25	2.78	1.53	1.395	0.783	-0.006	-0.795	0.46	0.01	0.39	0.70	6081
41	6.03	5.51	3.47	1.51	1.322	0.785	-0.080	-0.785	0.08	0.25	0.67	0.73	5809
42	6.27	4.59	2.46	1.50	1.530	0.785	-0.052	-0.785	0.54	0.21	0.64	0.79	6176
43	6.17	4.27	2.79	1.56	1.311	0.785	-0.120	-0.785	0.42	0.67	0.26	0.27	5770
44	6.05	6.29	2.80	2.03	1.270	0.785	-0.006	-0.785	0.43	0.70	0.23	0.28	5735
45	0.00	0.00	0.00	0.00	1.534	0.785	0.000	-0.785	0.51	0.20	0.65	0.76	6122

Discussion of the selected gait:

The value of the leg location variables for optimization run #15 are $r_{R1} = 0.057m$, $r_{R2} = 0.05m$, $r_{R3} = 0.032m$, $r_{R4} = 0.016m$, $\phi_{R1} = 84.2^\circ$, $\phi_{R2} = 45^\circ$, $\phi_{R3} = 0$, $\phi_{R4} = -45^\circ$,

For the anterior legs $R1, R2, L1, L2$, the value of r is much larger than that for the posterior legs $R3, R4, L3, L4$. This is because these legs are in the front and need to stretch out initially to pull

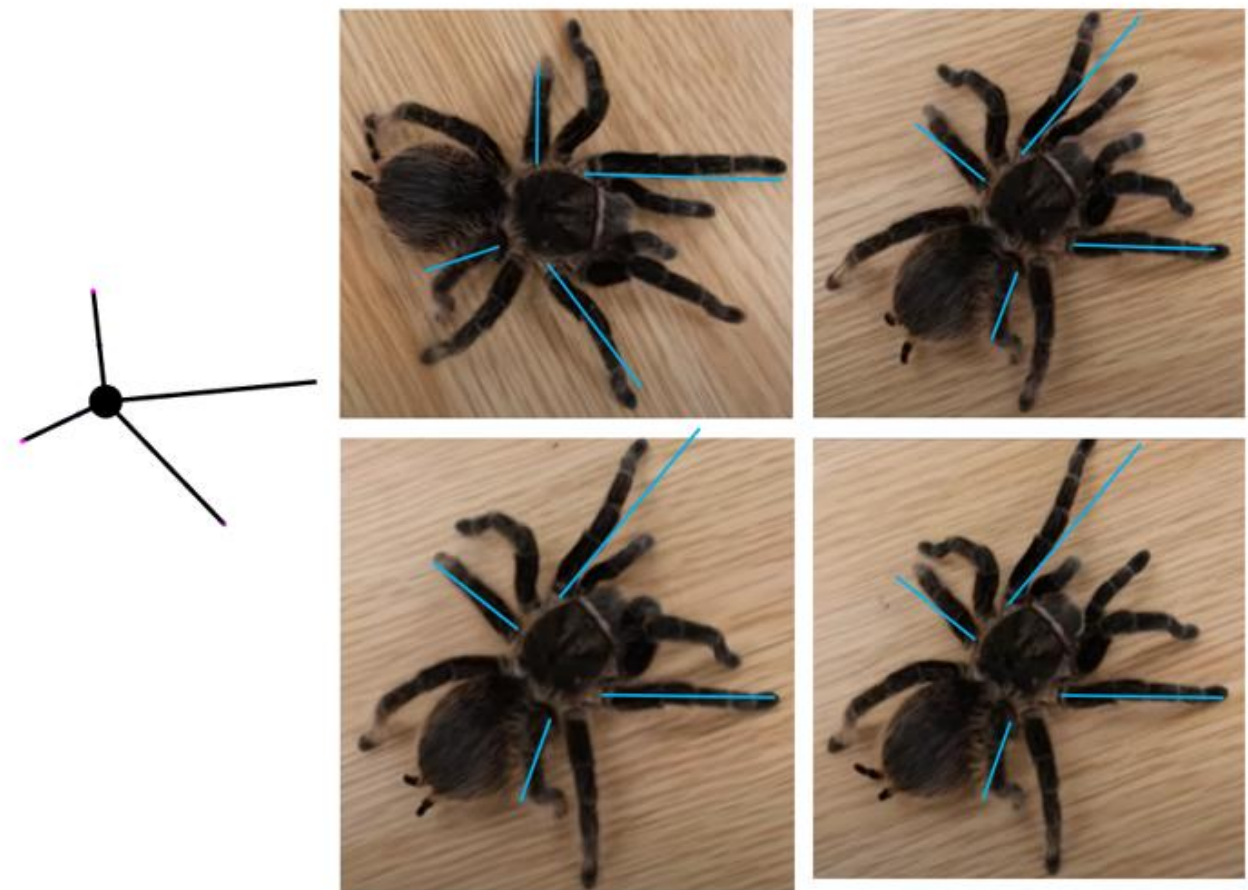


Figure 13: Leg position maps when the last leg of the leg group contacts the ground. Figure on the left shows the leg positions when leg $L1$ is placed on the ground obtained using least effort. Figures on the right show screenshots of 4 different strides performed by a tarantula taken from an online video [29]. In each of the 4 cases, leg $R4$ was the last to contact the ground and the screenshot was taken at this instant. The blue lines are transformed from the black lines (showing the legs) on the left, while preserving the length ratios and angles between the lines.

the body forward (and hence retract as the body moves ahead) while the legs in the back need to contract initially to push the body forward (and hence extend as the body moves ahead). As far as the value of ϕ is concerned, it is at the joint limits for legs 2, 3 and 4. For leg 1 it is about 16° off from the front direction. For comparison, we use a video of a tarantula walking on flat surface that was uploaded on YouTube [29]. In this video, the spider executes the alternating tetrapodal gait. We took 4 snapshots of different strides performed in the video and they were taken when the last of the legs L1, R2, L3, R4 was placed on the ground for that stride. These snapshots are shown in Figure 13 on the right. The stick diagram on the left shows a snapshot of the top view of optimization run 15 revealing legs L1, R2, L3, R4 working in coordination. Again, the image shows the time step when the last of these legs was placed on the ground. The black leg lines in the stick diagram were transformed into blue lines by scaling and rotating them for each image on the right to compare the position of the feet with those from the video. The angles between the leg lines and their length ratios are preserved in the blue lines. The comparison shows a lag in the gait obtained from run 15 for legs L1 while a lead for legs L3 and R4. One of the reasons this happens is because legs R4 and L3 are placed later on the ground in the video while in our derived gait Leg L1 is placed later.

The remaining 4 variables of run 15 that determine the time when the legs are placed on the ground are representative of the alternate-tetrapodal walking gait pattern as seen in nature. Figure 14 a, b and c represent gait pattern diagrams adapted from 3 different papers [22,23,24] and 14 d shows the gait obtained from our calculations where the solid lines represent a stance phase and blanks represent the swing phase. Each of the first 3 diagrams were observed in different species of tarantulas and are representative of the alternating tetrapodal gait. It can be noted that legs R1 and L1 are placed relatively later in our case compared to the other gaits. Some of this may be attributed

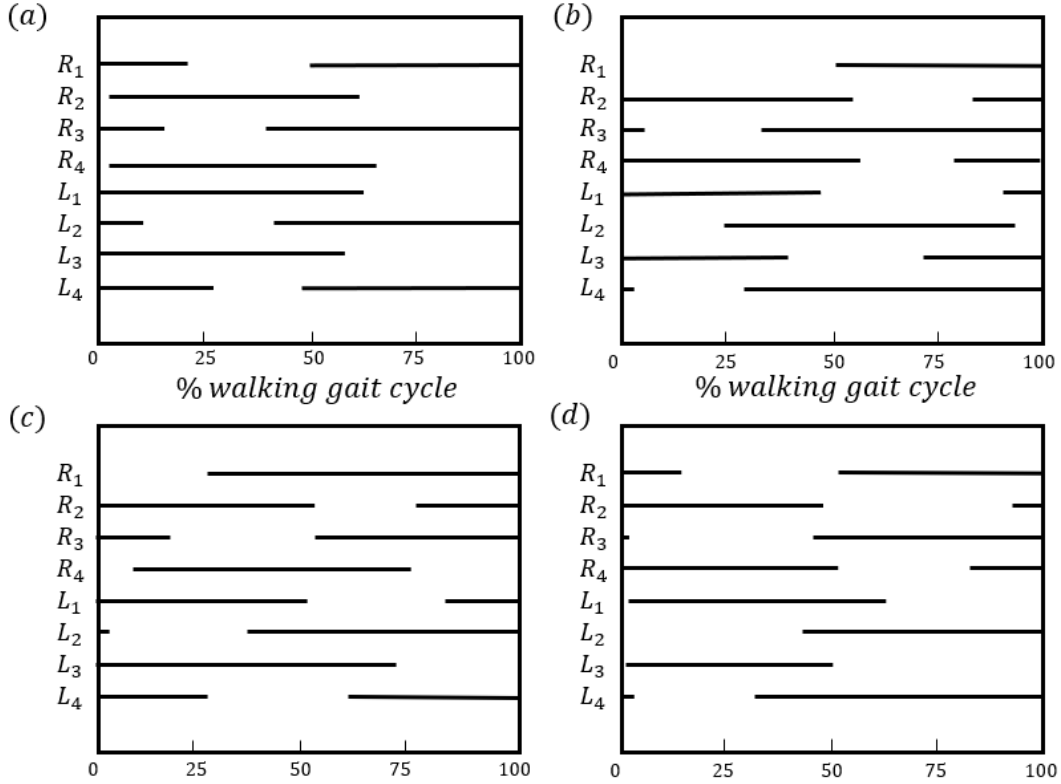


Figure 14: Gait phase diagrams of tarantulas from 4 different sources. (a) Gait phase diagram obtained from least effort. (b) Adapted from [22], (c) Adapted from [23], (d) Adapted from [24]. Solid Lines represent the stance phase while blanks represent the swing phase.

to the inaccuracies and approximations of the model. However, we believe the primary reason behind this is the omission of the role of pedipalps in the walking motion which may cause the fore legs to remain in contact for longer in the current cycle before they protract for the next one. Finally, we represent all the joint angles graphs for the 4 right legs for run 15 that are exhibited during the walking gait cycle of the spider in Figure 15. The legs on the left would exhibit the same joint angles with a phase shift of $T_{cycle}/2$. A video simulation of the walking gait is also available [30]. The simulation was carried out on the Gazebo simulator which is a physics engine used in various robotic simulations. Our model was created on a solid modelling software called *Solidworks* and its URDF consisted of 32 joints and 24 leg links and a body link. The joint angles

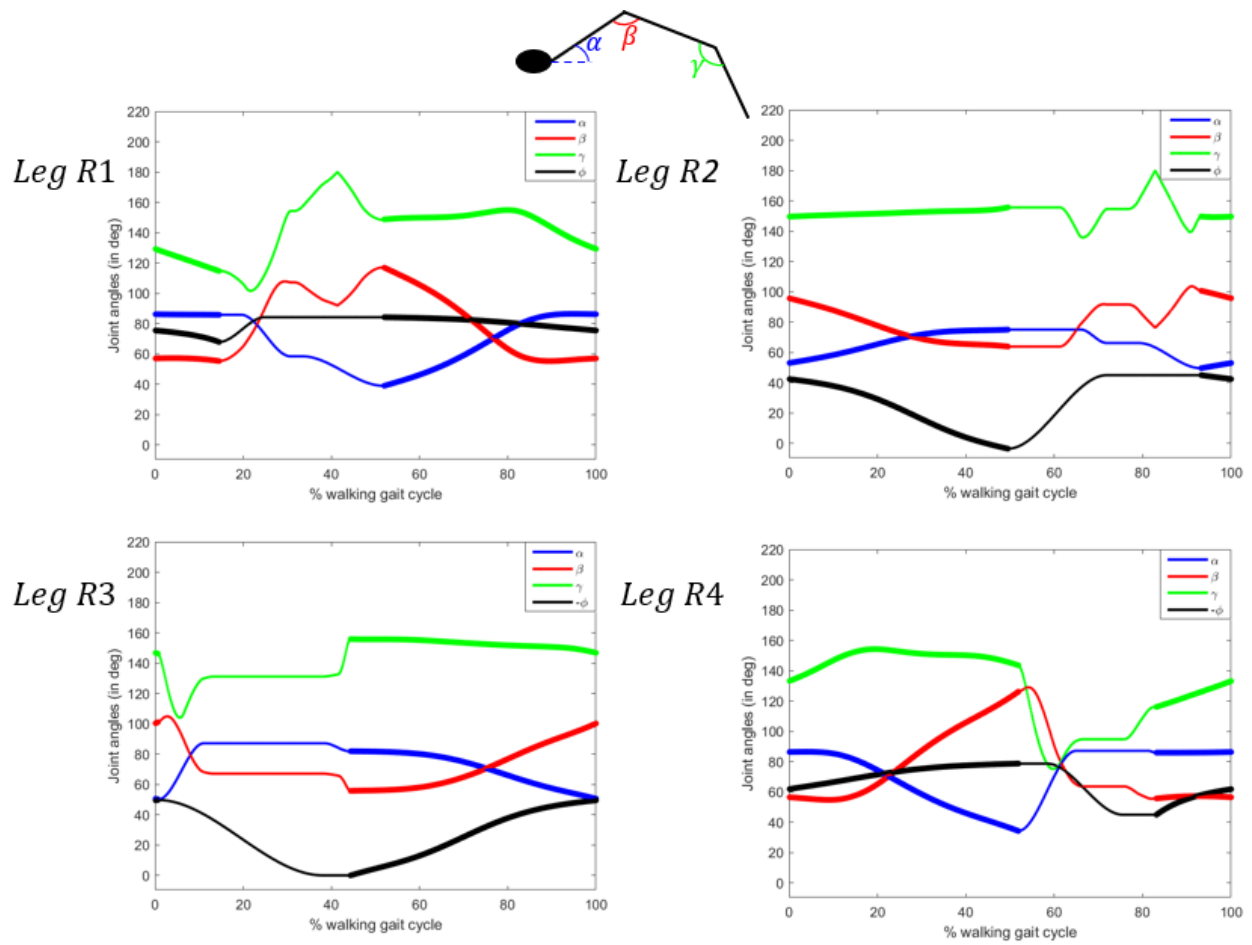


Figure 15: Joint angles during the walking gait cycle for legs R1, R2, R3 and R4. Bold lines indicate stance phase while thin lines indicate swing phase.

were communicated and controlled using the Robot Operating Software (ROS), thus resulting in the walking motion of the tarantula.

4. Conclusions

In this work we presented a hierarchical approach for deriving motions for a tarantula robot that not only has redundant legs but also redundant joints in each leg. Each motion was defined through optimization with an objective of minimizing the total joint efforts in the tarantula as it walks on a plane, horizontal surface. The reason for using this objective function was to obtain fluid and biologically realistic motions for the robot, so it resembles an actual tarantula while walking. The procedure we used was hierarchical in nature and the problem was broken down into a number of subproblems or stages, where in we started with studying the dynamics of one link, then moved on to a complete leg and then considered the spider as a whole. Many of these subproblems were formulated as Least-effort problems or LEPs to derive some physical parameter for the spider which could then be used for the next stage. The Final Optimization Problem was used to derive the complete walking gait for the spider with all the joint angles to define the motions performed during the stance phase and the swing phase. The motions obtained from the FOP were then compared with actual tarantula data to gauge how well, the least-effort principle could predict the motions compared to those observed in nature. We found a close relation between the derived walking gaits and the actual walking gaits and believe that the least-effort principle plays an important role in the decision-making process of a tarantula while walking.

The hierarchical framework defined in this work can be further extended to derive even more complex actions such as walking on uneven terrain, jumping etc. and each of the subproblems can be adapted to various cases. For example, if the spider wants to avoid obstacles, it may need to raise its feet higher than usual, and this new motion can be quickly derived using LEP 1. When the spider is walking on uneven terrain, a new dimension of height can be added to LEP 3 for each foot, to derive the ground plane forces on the feet that are all basically now at different elevations.

REFERENCES

- [1] Hussein, A., Gaber, M. M., Elyan, E., & Jayne, C. (2017). Imitation learning: A survey of learning methods. *ACM Computing Surveys (CSUR)*, 50(2), 1-35.
- [2] Zhu, Y., Wang, Z., Merel, J., Rusu, A., Erez, T., Cabi, S., ... & Heess, N. (2018). Reinforcement and imitation learning for diverse visuomotor skills. *arXiv preprint arXiv:1802.09564*.
- [3] Martin, B. J., & Bobrow, J. E. (1999). Minimum-effort motions for open-chain manipulators with task-dependent end-effector constraints. *The international journal of robotics research*, 18(2), 213-224.
- [4] Chettibi, T., Lehtihet, H. E., Haddad, M., & Hanchi, S. (2004). Minimum cost trajectory planning for industrial robots. *European Journal of Mechanics-A/Solids*, 23(4), 703-715.
- [5] Song, J., Qu, X., & Chen, C. H. (2016). Simulation of lifting motions using a novel multi-objective optimization approach. *International Journal of Industrial Ergonomics*, 53, 37-47.
- [6] Liu, C. K., Hertzmann, A., & Popović, Z. (2005). Learning physics-based motion style with nonlinear inverse optimization. *ACM Transactions on Graphics (TOG)*, 24(3), 1071-1081.
- [7] Felis, M. L., & Mombaur, K. (2012, November). Using optimal control methods to generate human walking motions. In *International Conference on Motion in Games* (pp. 197-207). Springer, Berlin, Heidelberg.
- [8] Nubar, Y., & Contini, R. (1961). A minimal principle in biomechanics. *The bulletin of mathematical biophysics*, 23(4), 377-391.
- [9] Jiang, Y., Van Wouwe, T., De Groote, F., & Liu, C. K. (2019). Synthesis of biologically realistic human motion using joint torque actuation. *ACM Transactions On Graphics (TOG)*, 38(4), 1-12.
- [10] Bobrow, J. E., Martin, B., Sohl, G., Wang, E. C., Park, F. C., & Kim, J. (2001). Optimal robot motions for physical criteria. *Journal of Robotic systems*, 18(12), 785-795.
- [11] Deo, A. S., & Walker, I. D. (1997). Minimum effort inverse kinematics for redundant manipulators. *IEEE Transactions on Robotics and Automation*, 13(5), 767-775.
- [12] Peng, X. B., Coumans, E., Zhang, T., Lee, T. W., Tan, J., & Levine, S. (2020). Learning agile robotic locomotion skills by imitating animals. *arXiv preprint arXiv:2004.00784*.

- [13] Bharatharaj, J., Huang, L., & Al-Jumaily, A. (2015, December). Bio-inspired therapeutic pet robots: Review and future direction. In *2015 10th international conference on information, communications and signal processing (icics)* (pp. 1-5). IEEE.
- [14] Robinson, H., MacDonald, B., & Broadbent, E. (2014). The role of healthcare robots for older people at home: A review. *International Journal of Social Robotics*, 6(4), 575-591.
- [15] Lakatos, G., Wood, L. J., Syrdal, D. S., Robins, B., Zaraki, A., & Dautenhahn, K. (2021). Robot-mediated intervention can assist children with autism to develop visual perspective taking skills. *Paladyn, Journal of Behavioral Robotics*, 12(1), 87-101.
- [16] "T8X," 2015. [Online]. Available: <http://www.robugtix.com/t8x/>
- [17] Grzelczyk, D., & Awrejcewicz, J. (2019). Modeling and control of an eight-legged walking robot driven by different gait generators. *International Journal of Structural Stability and Dynamics*, 19(05), 1941009.
- [18] Neubauer, W. (1994, September). A spider-like robot that climbs vertically in ducts or pipes. In *Proceedings of IEEE/RSJ International Conference on Intelligent Robots and Systems (IROS'94)* (Vol. 2, pp. 1178-1185). IEEE.
- [19] Lysenko, V., Mintchenia, W., & Zimmermann, K. (2007). Minimization of the number of actuators in legged robots using biological objects. In *Computer science meets automation: 52. IWK, Internationales Wissenschaftliches Kolloquium; proceedings; 10-13 September 2007; Volume I* (Vol. 52, pp. 483-488).
- [20] Karydis, K., Poulakakis, I., & Tanner, H. G. (2012, October). A switching kinematic model for an octapedal robot. In *2012 IEEE/RSJ International Conference on Intelligent Robots and Systems* (pp. 507-512). IEEE.
- [21] Chen, X., Wang, L. Q., Ye, X. F., Wang, G., & Wang, H. L. (2013). Prototype development and gait planning of biologically inspired multi-legged crablike robot. *Mechatronics*, 23(4), 429-444.
- [22] Biancardi, C. M., Fabrica, C. G., Polero, P., Loss, J. F., & Minetti, A. E. (2011). Biomechanics of octopedal locomotion: kinematic and kinetic analysis of the spider *Grammostola mollicoma*. *Journal of Experimental Biology*, 214(20), 3433-3442.
- [23] Wilson, D. M. (1967). Stepping patterns in tarantula spiders. *Journal of Experimental Biology*, 47(1), 133-151.

- [24] Hao, X., Ma, W., Liu, C., Li, Y., Qian, Z., Ren, L., & Ren, L. (2019). Analysis of spiders' joint kinematics and driving modes under different ground conditions. *Applied bionics and biomechanics*, 2019.
- [25] Foelix, R. (2011). *Biology of spiders*. OUP USA.
- [26] Vidoni, R., & Gasparetto, A. (2011). Efficient force distribution and leg posture for a bio-inspired spider robot. *Robotics and Autonomous Systems*, 59(2), 142-150.
- [27] Silva-Pereyra, V., Fábrega, C. G., Biancardi, C. M., & Pérez-Miles, F. (2019). Kinematics of male *Eupalaestrus weijenberghi* (Araneae, Theraphosidae) locomotion on different substrates and inclines. *PeerJ*, 7, e7748.
- [28] Wang, Z., Wang, J., Ji, A., Li, H., & Dai, Z. (2011). Movement behavior of a spider on a horizontal surface. *Chinese science bulletin*, 56(25), 2748-2757.
- [29] Alex Dixon. Tarantula Walk Cycle (Oct. 5, 2013). Accessed: Feb. 16, 2021. [Online Video]. Available: <https://www.youtube.com/watch?v=5eABaBg-Tyc>
- [30] Huzefa Lightwala. Gazebo simulation of a walking spider robot View 1 (Oct. 24, 2021). Accessed: Oct. 24, 2021. [Online Video]. Available: https://youtu.be/_Yv0VdNYtwk